A scenario optimization approach to reliability-based and risk-based design: Soft-constrained modulation of failure probability bounds

Reliability Engineering and System Safety 216 (2021) 107900

Contents lists available at ScienceDirect

Reliability Engineering and System Safety

journal homepage: www.elsevier.com/locate/ress

A scenario optimization approach to reliability-based and risk-based design: Soft-constrained modulation of failure probability bounds

Roberto Rocchetta [a,*], Luis G. Crespo [b]

[a] Department of Mathematics and Computer Science, Security W&I, Technical University of Eindhoven, Eindhoven, The Netherlands
[b] Dynamic Systems and Control Branch, NASA Langley Research Center, Hampton, VA, USA

ARTICLE INFO

Keywords:
Reliability-based design optimization
Scenario theory
Reliability bounds
Conditional value-at-risk
Constraints relaxation
Lack of data uncertainty
Convex programs

ABSTRACT

Reliability-based design approaches via scenario optimization are driven by data thereby eliminating the need for creating a probabilistic model of the uncertain parameters. A scenario approach not only yields a reliability-based design that is optimal for the existing data, but also a probabilistic certificate of its correctness against future data drawn from the same source. In this article, we seek designs that minimize not only the failure probability but also the risk measured by the expected severity of requirement violations. The resulting risk-based solution is equipped with a probabilistic certificate of correctness that depends on both the amount of data available and the complexity of the design architecture. This certificate is comprised of an upper and lower bound on the probability of exceeding a value-at-risk (quantile) level. A reliability interval can be easily derived by selecting a specific quantile value and it is mathematically guaranteed for any reliability constraints having a convex dependency on the decision variable, and an arbitrary dependency on the uncertain parameters. Furthermore, the proposed approach enables the analyst to mitigate the effect of outliers in the data set and to trade-off the reliability of competing requirements.

1. Introduction

Reliability-Based Design Optimization (RBDO) methods seek engineering designs that are both economically profitable and meet the desired safety and functionality requirements with high probability. Reliability requirements are generally prescribed as a set of inequality constraints and define specific conditions beyond which the design no longer fulfills relevant criterion on its safety and functionality [1–3]. These constraints depend on random variables describing sources of uncertainty and on design parameters the analyst can control. For instance, the geometry of a component must be selected to minimize manufacturing costs while ensuring a minimum probability of not exceeding a maximum load level given uncertain material properties.

A traditional approach to solve RBDO problems involves two nested loops, an outer loop searches for an optimal design whereas an inner loop evaluates manufacturing costs and failure probabilities of the optimal candidates [4]. Nested loop methods are often computationally very demanding because of the time-consuming estimation of the failure probability. Moreover, the cost of the design and its reliability often define conflicting objectives and thus, an unconstrained maximization of the failure probability might lead to expensive solutions [5]. To overcome these difficulties, numerically efficient and chance-constrained reformulations of RBDO problems is advisable.

A numerically efficient RBDO procedure can be achieved by replacing the nested loop with efficient alternatives, such as decoupled approaches [6], single-loop methods [7–9], or efficient approximations of the inner loop probabilistic estimation. Single-loop methods combine the outer loop and inner loop by substituting the reliability analysis with an approximation [10] whilst decoupled methods transform the nested loop optimization in a sequence of deterministic programs, see e.g., [11,12] for a more detailed discussion. Efficient reliability assessment methods have been proposed to reduce the computational cost of the inner loop like subset simulation methods [13], line sampling [14], importance sampling [15], first-order and second-order reliability methods [4,16–19], multi-fidelity surrogate-modeling strategies [20–23] and many others [24–26].

Chance-Constrained Programs (CCPs) [27] minimize the cost of a design while imposing probabilistic constraints defining a minimum acceptable reliability level. CCPs are generally Nondeterministic Polynomial-time hard (NP-hard), non-convex [28] and, thus, numerically hard to solve. The intractability of CCPs has motivated researchers to develop alternative solution techniques, like convexification approaches based on the Conditional-Value-at-Risk (CVaR). The CVaR is a coherent risk measure and measures the risk associated with a design solution by combining the probability of undesired events

* Corresponding author.
E-mail addresses: r.rocchetta@tue.nl (R. Rocchetta), luis.g.crespo@nasa.gov (L.G. Crespo).

https://doi.org/10.1016/j.ress.2021.107900
Received 10 December 2020; Received in revised form 23 June 2021; Accepted 29 June 2021
Available online 16 July 2021

Nomenclature

$\mathbf{d} \in \Theta$	Vector of n_d design parameters bounded in a set Θ
$\mathbf{x} \in \Omega$	Vector of $n_\mathbf{x}$ uncertain factors
$f_\mathbf{x}$	Joint probability density of $\mathbf{x}$
$J(\mathbf{d})$	Cost function
$\mathcal{F}$	Composite failure domain
$\mathcal{F}^j$	Failure domain for requirement $j = 1, \ldots, n_g$
g_j	Reliability performance function for requirements $j = 1, \ldots, n_g$
w	Worst-case reliability performance function
F_w	Cumulative distribution for w
$\hat{F}_w$	Empirical cumulative distribution for w
α	A probabilistic level
VaR_α	Value-at-risk at level α
$CVaR_\alpha$	Conditional VaR at level α
P_f	True failure probability for all requirements
$P_{f,j}$	True failure probability for the j^{th} requirement
R	True reliability for all requirements
V	Probability of scenario constraint violation
$\hat{R}$	Estimator of the reliability
$\mathcal{D}_N$	Data set of N samples of the uncertain factors
$[\underline{\epsilon}, \overline{\epsilon}]$	Bounds on the violation probability for all requirements
$[\underline{\epsilon}_j, \overline{\epsilon}_j]$	Bounds on the violation probability for requirement j
λ	The value-at-risk in a scenario program
ρ	Parameter weighting the cost of scenario constraints violations
$\zeta^{(i)}$	A slack variable for sample i
$\zeta_j^{(i)}$	A slack variable for sample i and the j^{th} requirement
β	Confidence parameter
$s_N^\star$	Number of support scenarios for all requirements
$v_{N,j}^\star$	Number of support scenarios for the j^{th} requirement
Θ	Design space
Θ_α^{VaR}	Set of feasible designs for a VaR constraint at a level α
Θ_α^{CV}	Set of feasible designs for a CVaR constraint at a level α
$\Theta_{\mathbf{x}^{(i)}}$	Set of designs satisfying a constraint imposed by $x^{(i)}$
Θ^{SP}	Set of feasible designs of a scenario program

with a measure of the magnitude/severity of these events. CVaR methods have been broadly used in portfolio optimizations, statistical machine learning and also in engineering design problems [29,30]. Replacing failure probability constraints with CVaR constraints can improve the numerical tractability of RBDO programs [31]. In facts, CVaR constraints are convex for convex reliability functions and offer control over a portion of the tails of distributions beyond a single quantile. However, one of the main drawbacks of a CVaR constraint versus a failure probability constraint is that the former is statistically less stable, i.e., an outlier can significantly change the value of the estimated CVaR.

In addition to these computational issues with RBDO and CVaR-based CCPs, the majority of the existing methods rely on a precise characterization of a probabilistic model, which is used to estimate failure probabilities and tail expectations. The prescription of a specific probabilistic model generally involves calibrating a joint Probability Distribution Function (PDF), a correlation/dependency structure, and the definition of a good model for the tails. Selecting a good model of the uncertainty can be challenging, especially for high-dimensional problems, or when dependencies are unknown, or due to data scarcity [32,33]. Poorly chosen uncertainty models can lead to designs that grossly under-perform in practice [33] and, in the worst-case, that are susceptible to severe failures [31,34]. For examples, consider a probabilistic model that underestimates the tails and a design obtained by minimizing a CVaR estimated using this probabilistic model. The optimized design will be likely susceptible to failures of unexpectedly high magnitude. Another example is the Nataf transformation, often used in RBDO to map a model of the uncertainty to the standard unit space. The Nataf transformation entails a specific assumption on the dependence structure of the uncertain factors [35]. However, under a lack of data, a specific dependency assumption is hard to justify and unwarranted because of its biasing effect on the final solution. The works of R. Lebrun and A. Dutfoy [35,36] present a detailed discussion on these issues when the Nataf transformation is applied to solve FORM and SORM problems.

If a lack of data is affecting the analysis, a non-probabilistic model or a mixture of non-probabilistic and probabilistic models offer a more robust alternative [37,38]. Evidence theory [39,40], possibility theory [41], credal sets, fuzzy sets and ambiguity sets theory [42–45], are some of the most used paradigms for this [46]. Distributionally robust CCPs have been proposed to identify robust designs that satisfy probabilistic constraints for a whole set of uncertainty models [47–49]. The authors of [50] present a hybrid reliability optimization method for handling imprecision via a combination of fuzzy and probabilistic uncertainty models. Similarly, [51,52] introduced a hybrid time-variant reliability measure and convex sets characterize the uncertain factors non-probabilistically whilst [38,53] proposed a set-valued description of the uncertain factors and a non-probabilistic reliability index for RBDO. Approaches that integrate CCP with the available data and without prescribing a model (or a set of modes) for the uncertainty are just starting to be explored.

Scenario optimization theory offers a powerful mathematical framework to solve CCPs according to data while prescribing generalization error bounds on the optimized design solutions. Generalization error bounds, also known as certificates of probabilistic performance, are computed based on the number of available samples, a confidence level selected by the analyst, and a statistical measure of the complexity of the decision. Scenario theory has been extensively studied for convex optimization programs [54–58] and recently extended to non convex cases [59–61]. Scenario theory has been applied to tackle prediction, regression [62], machine learning [63,64], robust design [65], and optimal control problems [66]. The use of scenario optimization for RBDO is fairly new. In [1] the authors developed a Scenario-RBDO framework to solve convex and non-convex reliability optimization problems. A powerful prospective certificate of generalization has been proposed for the resulting design, i.e., an upper bound on the probability of facing a future, not yet observed, failure with a magnitude greater than the historically recorded worst-case. However, this result focuses on extreme cases and a prospective bound on the failure probability was not provided.

In this work, we extend the approach of [1] to equip solutions of convex RBDO problems with upper and lower bounds on both the probability of failure and on the probability of extreme failures. A novel soft-constrained scenario program for RBDO and risk-based design is proposed based on the theoretical results in [67]. In contrast to hard-constrained programs for which all constraints must be satisfied with no exceptions, the fulfillment of soft constraints is preferred but not required. An optimal design is thus prescribed by minimizing a weighted sum of the cost of the design and penalty terms for constraint violations. For instance, an optimal design will minimize both the operational costs of a system and penalty terms associated with the severity of failures. The proposed scenario program shares similar benefits when compared to a traditional work of Rockafellar et al. [31] on buffered failure probabilities and CVaR-based reliability optimization. In contrast to the CVaR approach, a prospective reliability certificate for the optimized design can be obtained from the approach printed in this work. This certificate bounds the probability of exceeding a predefined Value-at-Risk (VaR) level. This certificate is obtained directly from the available data and without the need to prescribe a model (or a set of models) of the uncertainty. Thus, it is exempt from the subjectivity caused by having to prescribe an uncertainty model from insufficient data. In contrast to [1], the applicability of these bounds are restricted to RBDO problems which can be assumed convex in the space of decision variables. Nonetheless, the prescribed bounds are tighter (more informative) than the one obtained in [1], thus offering an improved quantification of the epistemic uncertainty affecting the reliability of the optimized design.

The main contributions of this work can be summarized as follows:

- The proposed method prescribes a design solution by minimizing a combination of the expected severity of failures (risk) and the design cost.
- Scenario theory is used to derive upper and lower bounds on the probability of exceeding a value-at-risk (a quantile) level. A reliability interval is derived selecting an appropriate VaR level.
- The reliability interval is derived without the need to prescribe a model for the uncertain parameters according to the available data only. The width of the interval quantifies the epistemic uncertainty (for lack of samples) affecting the reliability of a design.
- The soft-constrained optimization method can be used on any reliability problem whilst the reliability bounds can be applied by assuming the convexity of the RBDO problem. The number of uncertain parameters and the dependency of the reliability functions on these parameters can be arbitrary.
- The proposed approach can be used to trade-off the design's cost against reliability of some or all requirements.

The remainder of this paper is organized as follows: Section 2 presents the mathematical background on RBDO and CVaR approximation. Section 3 introduces Scenario optimization theory and theoretical robustness guarantees. In Section 4 the newly proposed scenario RBDO programs are presented. Section 5 exemplifies the method on an easily reproducible case study and Section 6 tests the applicability of the method on two realistic engineering examples. Section 7 closes the paper with a discussion on the results.

2. Mathematical background

A reliability CCP seeks an optimal design which minimizes a cost function while constraining the probability of failure below a threshold level:

$$\mathbf{d}^\circ = \arg\min_{\mathbf{d}\in\Theta} \left\{ J(\mathbf{d}) : P_f < 1-\alpha \right\}, \tag{1}$$

$$P_f = \int_{\mathcal{F}(\mathbf{d})} f_{\mathbf{x}}(\mathbf{x}) d\mathbf{x}, \tag{2}$$

where $0 \le \alpha \le 1$ is a target reliability level constraining the failure probability, $\mathbf{d}$ is a vector of design parameters constrained in a closed convex set $\Theta \subset \mathbb{R}^{n_d}$, $J(\mathbf{d}) : \mathbb{R}^{n_d} \to \mathbb{R}$ is a convex cost function, and $\mathbf{d}^\circ$ is the vector of optimized design parameters. The failure probability $P_f(\mathbf{d})$ in Eq. (2) is a multidimensional integral of the uncertainty model, $f_{\mathbf{x}}(\mathbf{x})$, a joint Probability Density Function (PDF) of uncertain parameters $\mathbf{x} \in \Omega \subseteq \mathbb{R}^{n_{\mathbf{x}}}$, computed over the composite failure domain $\mathcal{F}(\mathbf{d})$. This domain is defined as the union of n_g reliability requirements,

$$\mathcal{F}(\mathbf{d}) = \bigcup_{j=1}^{n_g} \mathcal{F}^j(\mathbf{d}) \tag{3}$$

where,

$$\mathcal{F}^j(\mathbf{d}) = \left\{ \mathbf{x} \in \Omega : g_j(\mathbf{d},\mathbf{x}) \ge 0 \right\}, \tag{4}$$

are the individual failure regions defined by the *reliability functions* $g_j : \mathbb{R}^{n_d} \times \mathbb{R}^{n_{\mathbf{x}}} \to \mathbb{R}$. A design $\mathbf{d}$ satisfies all requirements for a particular vector of uncertain variables $\mathbf{x}$ if $g_j(\mathbf{d},\mathbf{x}) < 0$ for all requirements $j \in \{1,\dots,n_g\}$. Note that $\alpha = 1$ in the optimization program (1) corresponds to an admissible failure probability equal to zero.

2.1. Chance constraints

The literature considered two types of chance-constraints: joint probabilistic constraints or individual probabilistic constraints [68,69]. The constraint in program (1) is called a joint chance constraint because it is composed of individual requirements that must be simultaneously satisfied with a prescribed probability. The constraint on the joint failure probability can be equivalently defined as follows:

$$P_f = \mathbb{P}\left[w(\mathbf{d},\mathbf{x}) \ge 0 \right] < 1-\alpha, \tag{5}$$

where

$$w(\mathbf{d},\mathbf{x}) = \max_{j\in\{1,\dots,n_g\}} g_j(\mathbf{d},\mathbf{x}), \tag{6}$$

is the *worst-case reliability function*. When $w(\mathbf{d},\mathbf{x}) < 0$ the design $\mathbf{d}$ satisfies all the reliability requirements for the uncertainty realization $\mathbf{x}$.

Alternatively to a joint chance constraint, each one of the n_g requirements can be associated to a specific probabilistic threshold α_j, thus defining the individual chance constraints as follows:

$$P_{f,j} = \mathbb{P}\left[g_j(\mathbf{d},\mathbf{x}) \ge 0 \right] < 1-\alpha_j, \quad j = 1,\dots,n_g, \tag{7}$$

where $P_{f,j}$ are the failure probability for requirement $j = 1,\dots,n_g$ and $0 \le \alpha_j \le 1$.

Note that If $\sum_{j=1}^{n_g} \alpha_j \le \alpha$, a feasible solution of individual constraints (7) is also feasible for the joint constraint (5). Hence, joint chance-constraints are significantly more stringent than individual constraints because the former must hold together with high probability whilst individual constraints have to be satisfied with separate probabilistic levels [70]. Joint probabilistic constraints are better suited to deal with problems where individual requirements describe a collective goal, e.g., the overall system reliability must be higher than a predefined threshold level. In contrast, individual constraints can be used when individual requirements describe separate objectives, e.g., when minimum reliability levels for the individual components must be provided.

2.2. Var formulation of the RBDO problem

An equivalent formulation of program (1) is,[1]

$$\mathbf{d}^\circ = \arg\min_{\mathbf{d}\in\Theta} \left\{ J(\mathbf{d}) : VaR_\alpha(w) < 0 \right\}, \tag{8}$$

where

$$VaR_\alpha(w) = \inf\{ w(\mathbf{d},\mathbf{x}) \in \mathbb{R} : \alpha \le F_w(w) \}$$

[1] The constraint $P_f(\mathbf{d}) < 1-\alpha$ implies $\mathbb{P}\left[w(\mathbf{d},\mathbf{x}) \ge 0 \right] < 1-\alpha$ which is equivalent to $VaR_\alpha(w) < 0$.

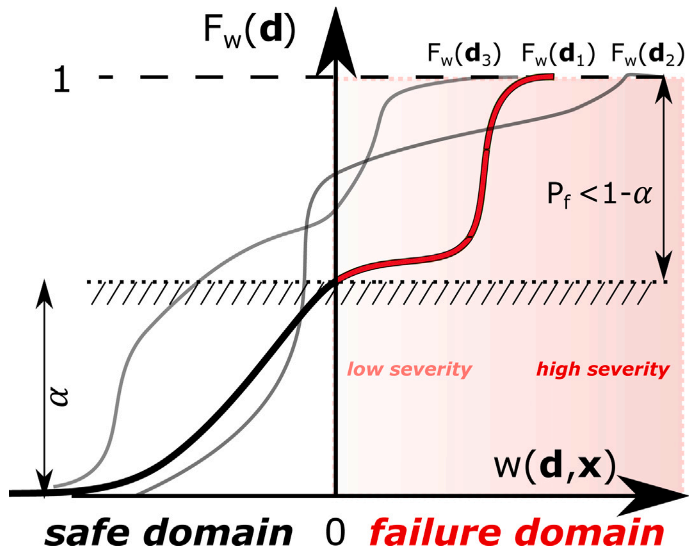

Fig. 1. CDFs of the worst-case performance w associated to three feasible designs, i.e., $\mathbf{d}$ for which $VaR_\alpha(w) \leq 0$. $\mathbf{d}_2$ is the most reliable but also the design exhibiting the most severe violations.

is the *Value-at-Risk* at level α, i.e., the inverse CDF of the distribution of $w(\mathbf{d}, \mathbf{x})$ for a predefined level α, induced by the design $\mathbf{d}$ and for the uncertainty model $f_\mathbf{x}$. Note that (8), differently from (1), imposes a constraint on the quantile function (a value of w) rather than on a probability.

A closed-form expressions for the quantile function is typically not available in VaR constraints require a numerical evaluation, e.g., using Monte Carlo Sampling (MCS). Hence, a solution of programs (1) and (8) is often computationally demanding to obtain because the multidimensional integral P_f must be estimated several times. Means to evaluate the failure probability through standard MCS are presented next. Given a set of N samples $\mathcal{D}_N = \left\{\mathbf{x}^{(i)}\right\}_{i=1}^N$ drawn from $f_\mathbf{x}$, the integral in (2) can be approximated by,

$$\hat{P}_f(\mathbf{d}) = \frac{1}{N}\sum_{i=1}^{N} \mathbf{1}_{\{w^{(i)}\geq 0\}}, \tag{9}$$

where $\mathbf{1}_{\{w^{(i)}\geq 0\}}$ is the indicator function for the failure condition $w(\mathbf{d}, \mathbf{x}^{(i)}) \geq 0$. Similarly, the empirical Cumulative Distribution Function (CDF) of w is computed by,

$$\hat{F}_w(W) = \frac{1}{N}\sum_{i=1}^{N} \mathbf{1}_{\{w^{(i)}\leq W\}}, \tag{10}$$

from which a VaR at level α can be readily computed. This estimates enable solving programs (1) and (8). Note however that the derivative discontinuities of these estimates complicate the usage of gradient-based optimization algorithms. Moreover, a large sample size N is generally required to improve accuracy and convergence of the estimators and an uncertainty model $f_\mathbf{x}$ is a key component in the MCS procedure.

2.3. Non-convexity of value-at-risk constraints

Let us define the feasibility set of the chance-constrained program (8), that is, the set of designs satisfying the VaR constraint for a given α level, as follows:

$$\Theta_\alpha^{VaR} = \left\{\mathbf{d} \in \Theta : VaR_\alpha(w) \leq 0\right\}.$$

A sufficient condition for the set Θ_α^{VaR} to be a convex is to have a mapping $\mathbf{d} \to P_f$ which is quasi-concave [71]. As example, if w is a quasi-convex function in $(\mathbf{d}, \mathbf{x})$ [72] and $\mathbf{x}$ has a log-concave density $f_\mathbf{x}$, the chance-constraint $P_f < 1 - \alpha$, admits a convex reformulation given by [71]

$$\log(P_f) < \log(1 - \alpha).$$

However, with the exception of log-concave $f_\mathbf{x}$ and a limited class of functions w, the set of designs satisfying the VaR constraint is non-convex. Therefore, chance-constrained optimization problems are generally non-convex, even when the reliability functions $g_j(\mathbf{d}, \mathbf{x})$ with $j = 1, \ldots, n_g$ are convex in the design space. This further complicates the tractability of this type of problems.

2.4. Severity of violations and risk-based design

Besides convexity issues, the constraint in (8) gives no guarantees on the severity of failures, i.e., the positive values of w can be arbitrarily large. If the value of the worst-case reliability function when $w > 0$ is a measure of the severity of the reliability violation, the analyst might want to control not only the failure probability, i.e., the integral over the right tail of the distribution of w, but also the shape of the upper tail of w. This design principle is also known in the literature as a risk-based design because both the probabilities of failure events and the severity of these events are accounted for while optimizing the design. This risk-based design criterion will be considered below. The severity of the violation, as measured by the value of w, is given by

$$\sigma(\mathbf{d}) = \mathbb{E}[w(\mathbf{d}, \mathbf{x}) | w(\mathbf{d}, \mathbf{x}) \geq 0], \tag{11}$$

where the severity function $\sigma(\mathbf{d})$ is the conditional expectation of $w(\mathbf{d}, \mathbf{x})$ over the failure region. This concept is depicted in Fig. 1 which shows an example of chance-constrained reliability problem. The CDFs of w for three designs are presented. The designs are feasible according the VaR constraint because satisfy the probabilistic constraint for the level α and $\mathbf{d}_1$ has the highest failure probability. However, $\mathbf{d}_2$ leads to the most severe violations.

2.5. CVaR approximation

CVaR, also known as expected shortfall or superquantile, has been used to approximate the chance constraint in (8) when the uncertainty models $f_\mathbf{x}(\mathbf{x})$ are continuous. CVaR is defined as [73]:

$$CVaR_\alpha(w) = \frac{1}{1-\alpha}\int_\alpha^1 F_w^{-1}(\tau)d\tau, \tag{12}$$

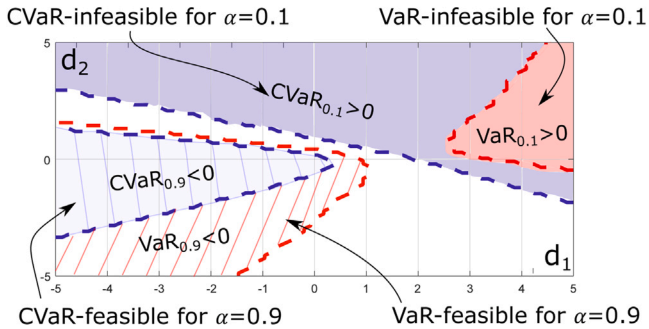

Fig. 2. Design spaces for the original chance constraint (red) and its convex relaxation (blue).

and for continuous distributions, $CVaR_\alpha(w)$ is an expectation over a 'portion' of the upper tail of the distribution of w, i.e., $CVaR_\alpha(w) = \mathbb{E}[w|w \geq VaR_\alpha(w)]$. Note the similarity between the CVaR and the severity metric $\sigma(\mathbf{d})$. The former coincides with the severity σ when the integration domain is defined over the composite failure region.[2] The CVaR may be non-negative for designs that satisfy the chance constraint in (8). On the other hand, thanks to the non-decreasing inverse CDF we have:

$$\int_\alpha^1 F_w^{-1}(\tau)d\tau > VaR_\alpha(w), \tag{13}$$

and, thus, a $CVaR_\alpha(w) \leq 0$ implies $VaR_\alpha(w) \leq 0$. Hence, if a design $\mathbf{d}$ satisfies a CVaR constraint at level α it also satisfies the constraint in (8).

A CVaR-constrained approximation of program (8) is defined as follows:

$$\mathbf{d}^\circ = \arg\min_{\mathbf{d}\in\Theta} \left\{ J(\mathbf{d}) : CVaR_\alpha(w) \leq 0 \right\}. \tag{14}$$

Note that when the reliability functions g are convex[3] in $\mathbf{d}$, the constraint $CVaR_\alpha(w) \leq 0$ gives the following convex inner approximation of the feasibility set Θ_α^{VaR} [74],

$$\Theta_\alpha^{CV} = \{\mathbf{d} \in \Theta : CVaR_\alpha(w) \leq 0\} \subseteq \Theta_\alpha^{VaR}.$$

Thus, a CVaR-constrained program is a convex program when the cost and reliability functions are convex in the design space. This convexification of the design space makes (14) conservative because a feasible designs of VaR program might not be feasible in (14). Hence, this formulation guarantees a conservative result in terms of failure probability, see e.g., [31].

Fig. 2 illustrate the feasible and infeasible design space of programs (8) and (14) for the linear reliability function $w = d_1 + x_1 - d_2 x_2$ with $\alpha = 0.1$ and $\alpha = 0.9$. Notice that the feasible design space Θ_α^{CV} of program the CVaR-constrained program is contained by the feasibility set Θ_α^{VaR} of program (8). Moreover, even for a linear w the feasible space Θ_α^{VaR} can result non-convex, e.g., the complement set of the VaR infeasible domain for $\alpha = 0.1$ shown in red color at the top right corner is non-convex.

For continuous distributions the conditional expectation coincides with the CVaR. In the general case, however, $CVaR_\alpha(w)$ is not equal to an average of outcomes greater than $VaR_\alpha(w)$ and an estimator obtained by averaging a fractional number of scenarios might result in discontinuities [34]. This complicates the solution of program (14) when gradient-based solvers are employed. A continuous sampling-based estimator of the CVaR can be obtained as a weighted average of a conditional expectation and VaR [34].

Program (14) has, however, some drawbacks:

1. CVaR estimation is sensitive to the uncertainty model $f_{\mathbf{x}}$, especially in the tails regions.
2. A CVaR constraint can be very stringent and the convex inner approximation of Θ_α^{VaR} might potentiality be empty.
3. For a non-convex function w in $\mathbf{d}$, a CVaR constraint is only convex in the space of $\mathbf{x}$.

In the next sections, we will provide background on Scenario optimization theory and a novel soft-constrained scenario program for RBDO and risk-based design proposed by the authors. This new methods can be used to overcome the first and second drawbacks of CVaR-constrained programs like (14). Similarly to CVaR methods, scenario programs are convex in the space of $\mathbf{x}$. In contrast with traditional method however, a model $f_{\mathbf{x}}$ is not required to solve scenario optimizations. Furthermore, the proposed soft-constrained scenario RBDO program always admits a feasible design (its feasibility set is always non-empty).

3. Scenario theory

Let us first outline the common structure used in scenario theory. Consider the probability space $(\Omega, \mathfrak{F}, \mathbb{P})$, where Ω is an event space equipped with a σ-algebra $\mathfrak{F}$ and a stationary probability measure $\mathbb{P}$ [65]. In practice, the probability $\mathbb{P}$ is unknown and only a data set $\mathcal{D}_N = \left\{\mathbf{x}^{(i)}\right\}_{i=1}^N \in \Omega^N$ containing N independent and identically distributed (IID) realization of the uncertain parameters is available and it belongs to the Cartesian product of the event space, $(\Omega^N, \mathfrak{F}^N, \mathbb{P}^N)$, also equipped with a σ-algebra and the N-fold probability measure $\mathbb{P}^N = \mathbb{P}\times\mathbb{P}\times\cdots\times\mathbb{P}$ (N-times). A scenario optimization program $\mathcal{SP}(\mathcal{D}_N)$ is a technique for obtaining solutions to CCPs based on a sample of the constraints. Each realization $\mathbf{x}^{(i)} \in \mathcal{D}_N$ is a *scenario*.

3.1. Scenario RBDO with joint constraints

A scenario RBDO program with joint constraints can be defined as follows:

$$\mathbf{d}^\star = \underset{d}{\operatorname{argmin}} \quad \left\{ J(\mathbf{d}) : \quad \mathbf{d} \in \Theta_{\mathbf{x}^{(i)}}, \quad \mathbf{x}^{(i)} \in \mathcal{D}_N \right\}, \tag{15}$$

where

$$\Theta_{\mathbf{x}^{(i)}} = \left\{ \mathbf{d} \in \Theta : w(\mathbf{d}, \mathbf{x}^{(i)}) \leq 0 \right\},$$

is the set of feasible designs induced by the ith scenario constraint and $\Theta^{\mathcal{SP}} = \bigcap_{i=1}^N \Theta_{\mathbf{x}^{(i)}}$ is the feasibility set for the scenario program with all the constraints in place. The set $\mathcal{D}_N$ defines N deterministic constraints which approximate a joint chance constraint in classical CCPs providing that the scenarios are realizations of the underlying uncertainty. As such, the scenarios might be obtained from available measurements (so no uncertainty model is needed), or they might be obtained from MCS. Differently from chance constrained programs like (8), the failure probability is replaced by N deterministic constraints on w, i.e., the set of feasible designs of (15) is comprised of design points for which the empirical failure probability is zero.

3.2. Scenario RBDO with individual constraints

The N scenario constraints in (15) offer a samples-based reformulation of the joint probabilistic constraint in Eq. (5). Analogously, individual chance constraints can be rewritten via an extended version of the scenario approach as described in [75]. Consider the following scenario RBDO program with multiple requirements:

$$\mathbf{d}^\star = \underset{\mathbf{d}}{\operatorname{argmin}} \left\{ J(\mathbf{d}) : \mathbf{d} \in \bigcap_{i=1}^N \Theta^j_{\mathbf{x}^{(i)}}, j = 1 \ldots, n_g \right\}, \tag{16}$$

[2] $CVaR_\alpha(w)$ is equal to $\sigma(\mathbf{d})$ for a probabilistic level $\alpha = 1 - P_f$ because, by definition, $VaR_{1-P_f}(w) = 0$.

[3] This implies that w is also convex as the maximum operator preserves convexity.

where

$\Theta^j_{\mathbf{x}^{(i)}} = \left\{ \mathbf{d} \in \Theta : g_j(\mathbf{d}, \mathbf{x}^{(i)}) \leq 0 \right\},$

is the feasibility set defined by the ith scenario for the requirement jth. Notice that the feasibility set in (15) can be equivalently defined as $\Theta_{\mathbf{x}^{(i)}} = \bigcap_{j=1}^{n_g} \Theta^j_{\mathbf{x}^{(i)}}$.

3.3. Basic assumptions and definitions

A scenario program may provide a feasible solution for a CCP but such solution is likely sub-optimal, and especially for a small sized data set $\mathcal{D}_N$ [76]. Nonetheless, an exact solution for CCPs can be only obtained when $f_{\mathbf{x}}$ is known with certainty. This only occurs asymptotically when $N \to \infty$ and, therefore, exact solutions to CCPs are generally unavailable in practice. Most importantly, scenario optimization programs lead to design solutions that are optimal for the available data while rendering probabilistic guarantees which reflect the lack of knowledge on the underlying $\mathbb{P}$. Scenario-based probabilistic guarantees, also known as prospective-reliability certificates, assess how well optimal designs $\mathbf{d}^\star$ performs against unseen samples drawn from the same data generating process [55]. These robust guarantees are formally derived from a few basic assumptions and definitions. For completeness sake, the most important concepts are presented next.

Assumption 1 (*Existence and Uniqueness*)**.** *The optimal design $\mathbf{d}^\star$ solution of $\mathcal{SP}(\mathcal{D}_N)$ exists and is unique for every data sequence $\mathcal{D}_N$* Existence of the solution may be lost when $J(\mathbf{d})$ improves as $\mathbf{d}$ drifts away toward infinity in some directions [57]. This behavior can be prevented by confining optimization to a compact domain Θ. If multiple optimal solutions exist in Θ a tie-break rule can be implemented, e.g. selecting the solution with minimum w among the set of equally suitable candidates (and possibly optimizing additional convex functions in $\mathbf{d}$).

Definition (*Violation Probability*)**.** *The probability*

$$V(\mathbf{d}^\star) = \mathbb{P}\left[\mathbf{x} \in \Omega : \mathbf{d}^\star \notin \Theta_{\mathbf{x}}\right], \tag{17}$$

is called violation probability. Given a reliability parameter $\epsilon \in [0,1]$, a design $\mathbf{d}^\star$ is called ϵ-robust (or ϵ-feasible) if $V(\mathbf{d}^\star) \leq \epsilon$, [58]. An ϵ-robust solution will comply with the requirements induced by new scenarios with probability no less than $1-\epsilon$. Means for evaluating ϵ according to the convexity of (15) are given in [55,58,60]. If the feasibility set is defined as in (15), $V(\mathbf{d}^\star)$ coincides with the true failure probability of $\mathbf{d}^\star$.

Definition (*Set of Support Constraints, or Support Set*)**.** *A support set $\mathcal{S} \subseteq \mathcal{D}_N$ is a k-tuple $\mathcal{S} = \{\mathbf{x}^{(i1)}, \ldots, \mathbf{x}^{(ik)}\}$ for which the solutions of scenario program $\mathcal{SP}(\mathcal{S})$ and program $\mathcal{SP}(\mathcal{D}_N)$ are identical.* The set $\mathcal{S}$ is of minimal cardinality when the removal of any of its elements makes the optimum of $\mathcal{SP}(\mathcal{S})$ different than the optimum of $\mathcal{SP}(\mathcal{D}_N)$. The cardinality of the set of support constraints $s^\star_N = |\mathcal{S}|$ defines the *complexity* of the solution and is a random quantity because it deepens on the random data set $\mathcal{D}_N$. Note that for convex optimization programs, $s^\star_N$ is capped by the dimension of the design space n_d, i.e., the complexity of a convex program is a-priori upper bounded. This can be derived from a basic argument using Helly's Theorem, [54]. A scenario program generally admits several support sets and the set with the smallest complexity renders the best prospective reliability bounds. If N individual scenario constraints are adopted as in program (16), a set of support constraints for individual requirements is denoted by $\mathcal{S}_j$ whilst its dimension by $v^\star_{N,j} = |\mathcal{S}_j|$. Notice that $\mathcal{S}_j$ is a collection of scenarios that when individually removed from a constraint on requirement j, improves the solution of the scenario program. The support set of (15) can be equivalently written as $\mathcal{S} = \bigcup_{j=1}^{n_g} \mathcal{S}_j$ [75].

Assumption 2 (*Non-degeneracy*)**.** *For any positive integer $N \in \mathbb{N}_0$ and data set $\mathcal{D}_N$, the solution of the scenario program $\mathcal{SP}(\mathcal{D}_N)$ coincides with probability 1 with the solution of $\mathcal{SP}(\mathcal{S})$* Non-degeneracy is a mild assumption for convex programs since support constraints are always active constraints (but the converse does not always remain true). In the general non-convex case however, $\mathcal{S}$ might include non-active constraints. For instance, the removal of a single non-active constraint can yield a new optimum having a smaller cost [1].

Definition (*Prospective-reliability*)**.** *The probability*

$$R(\mathbf{d}^\star) = \mathbb{P}\left[\mathbf{x} \in \Omega : w(\mathbf{d}^\star, \mathbf{x}) < 0\right], \tag{18}$$

is called prospective-reliability, i.e., the true reliability of $\mathbf{d}^\star$. When constraints are defined as in (15), an ϵ-robust solution is at least $(1-\epsilon)$-reliable.

Samples-based estimators of the violation probability are inherently stochastic, as they depend on the random set of scenarios $\mathcal{D}_N$. Nevertheless, it is proven that for convex scenario programs,[4] the distribution of $V(\mathbf{d}^\star)$ is dominated by a Beta distribution [55]. This result offers a way to monitor the robustness of the optimized design, i.e., an upper bound on $V(\mathbf{d}^\star)$ which quantifies the epistemic uncertainty arising from a lack of asymptotic convergence. However, a design solution of (15) must make the empirical failure probability based on the scenarios in $\mathcal{D}_N$ equal to zero. As such, limiting design architectures might either make (15) infeasible, or yield to overly-high cost values. In the next section, we adopt the constraints relaxation strategy proposed by [67] to overcome these issues.

4. The proposed methods for risk-based and reliability-based design: the soft-constrained scenario approach

In a previous work of the authors [1], a scenario approach to RBDO was proposed to identify a design which minimizes the α percentile of the worst-case reliability function, i.e., a program enforcing a constraint $VaR_\alpha(w) \leq \gamma$ where γ is a scalar cost to be minimized. Selecting an $\alpha = 1$, a certificate of robustness against extreme cases has been obtained [1] as follows:

$\mathbb{P}[w(\mathbf{d}^\star, \mathbf{x}) \geq \gamma^\star] \leq \epsilon(s^\star_N),$

where $\gamma^\star$ is the maximum value of the worst-case reliability function in correspondence of the optimum. This certificate ensures that, for any new scenario $\mathbf{x}$, the probability that $\mathbf{d}^\star$ will face a failure of magnitude greater than a worst-case given by $\gamma^\star = \max_i w(\mathbf{d}^\star, \mathbf{x}^{(i)})$ is, at worst, $\epsilon(s^\star_N)$. This is a powerful certificate of generalization which applies to the design solution of any scenario RBDO problem without restrictions on the functional form of w in the design space. However, the optimized $\gamma^\star$ is not controllable by the designers and, thus, the certificate does not provide guarantees on the failure probability $\mathbb{P}[w(\mathbf{d}^\star, \mathbf{x}) \geq 0]$. Moreover, only an upper bound on the violation probability was prescribed by the previous approach.

In contrast with [1], the new approach proposed in this work identifies an optimal design that minimizes a tail expectation (expected magnitude of failures) rather than $VaR_\alpha(w)$. Moreover, the new scenario RBDO formulation provides an upper and lower bounds on the probability $\mathbb{P}[w(\mathbf{d}^\star, \mathbf{x}) \geq \lambda]$, where λ a value-at-risk selected by the analysts. For instance, a $\lambda = 0$ can be selected to obtain a lower and an upper bond on the probability of failure of $\mathbf{d}^\star$. The lower and upper bounds are guaranteed to hold for convex scenario programs and, thus, we restrict the applicability of the approach to functions $w(\mathbf{d}, \mathbf{x})$ and costs $J(\mathbf{d})$ that are convex in $\mathbf{d}$. Thus, this can be used to prescribe stronger certificates (tighter epistemic bounds) on the probability of facing extreme cases, $\lambda > 0$, or on the probability of failure, $\lambda = 0$.

[4] Under the existence, uniqueness and non-degeneracy assumptions for any stationary $\mathbb{P}$ and N independent $\mathbf{x}$.

4.1. Scenario RBDO with joint soft constraints

Consider the scenario program:

$$\langle \mathbf{d}^\star, \zeta^\star \rangle = \arg \min_{\substack{\mathbf{d}\in\Theta \\ \zeta\geq\lambda}} \{ J(\mathbf{d}) + \rho \sum_{i=1}^{N} \left(\zeta^{(i)} - \lambda\right) : \\ w(\mathbf{d}, \mathbf{x}^{(i)}) \leq \zeta^{(i)},\ i = 1, \dots, N \}, \tag{19}$$

where $\zeta \in \mathbb{R}^N$ is a vector of slack variables associated to the N scenario constraints, $\rho > 0$ is a constant value used to penalize designs for which $w(\mathbf{d}, \mathbf{x}^{(i)})$ is positive, and $\lambda \in \mathbb{R}$ is a value-at-risk level which define a lower bound on the slack variables. Program (19) with $\lambda = 0$ seeks a design which minimizes a weighted sum of the $J(\mathbf{d})$ and individual reliability violations. This implies a reduction in both the empirical failure probability and in the severity of the violations as measured by $\sigma(\mathbf{d})$ in (11).

For $\lambda = 0$ all the non-zero terms in the vector $\zeta^\star$ correspond to scenarios falling into the failure region. The magnitude of $\zeta^{\star(i)} > 0$ is an indicator of the severity of the reliability violation, i.e., scenarios for which $\zeta^{(i)} = w(\mathbf{d}, \mathbf{x}^{(i)})$. In contrast, a $\lambda \neq 0$ defines a program that seeks an optimal design which minimizes a combination of cost and violation of the constraints $w \leq \lambda$. Hence, a $\lambda < 0$ means that program (19) is imposing a more stringent constraint that $w \leq 0$ on each scenario. Conversely, $\lambda > 0$ indicates a program that relaxes the requirements violation.

Note that the penalty terms in (19) enable the analyst to trade-off the empirical failure probability and the severity of point failures. It can be conveniently used to:

- Identify RBDO designs that are infeasible when the $w \leq 0$ are enforced as hard constraints.
- Shape the tail of the distribution of w falling into the failure domain.
- Trade-off reliability and cost by tuning ρ. When $\rho \to \infty$ the program goes back to the original formulation in (15), for which the constraints are hard.

4.2. Scenario RBDO with individual soft constraints

Program (19) weights all the reliability requirements equally. However, there might be requirements whose violation is more serious. For instance, the stability of a control system is regarded as more important than the need for a small control effort. To this end, we proposed a modified version of program (19) with multiple constraints:

$$\langle \mathbf{d}^\star, \zeta^\star \rangle = \arg \min_{\mathbf{d},\zeta} \{ J(\mathbf{d}) + \sum_{j=1}^{n_g} \rho_j \sum_{i=1}^{N} (\zeta_j^{(i)} - \lambda_j) : \\ g_j(\mathbf{d}, \mathbf{x}^{(i)}) \leq \zeta_j^{(i)},\ j = 1, \dots, n_g,\ i = 1, \dots, N, \\ \mathbf{d} \in \Theta,\ \zeta_j^{(i)} \geq \lambda_j,\ j = 1, \dots, n_g,\ i = 1, \dots, N \} \tag{20}$$

where the elements of the vector $\rho \in \mathbb{R}^{n_g}$ weight the magnitude of violations for individual requirements and a $\lambda_j < 0$ can be selected to tighten or relax the individual reliability requirements. Differently from (19), the terms ρ_j in program (20) can be used exercise a certain degree of control over individual failure modes and weight the n_g requirements differently.

4.3. Prospective-reliability bounds

The work of [67] provides a way to quantify the prospective-reliability of (19), which is an optimization program with soft scenario constraints.

Assumption 3 (*Non-accumulation*). *For every $\mathbf{d} \in \Theta$, it holds that $\mathbb{P}[\mathbf{x} \in \Omega : w(\mathbf{d}, \mathbf{x}) = a] = 0$, where a is a scalar value.* This assumption is generally satisfied when the scenario do not accumulate, i.e., when the uncertain factors $\mathbf{x}$ admit a probability density function.

Theorem 1. *Under Assumptions 1 and 3 and for any probability space and stationary $\mathbb{P}$ it holds that:*

$$\mathbb{P}^N[\underline{\epsilon}(s_N^\star) \leq V(\mathbf{d}^\star) \leq \overline{\epsilon}(s_N^\star)] \geq 1 - \beta \tag{21}$$

where $\underline{\epsilon}(s_N^\star)$ and $\overline{\epsilon}(s_N^\star)$ are lower and upper bounds on the violation probability $V(\mathbf{d}^\star) = \mathbb{P}[w(\mathbf{d}^\star, \mathbf{x}) \geq \lambda]$, $\beta \in [0, 1]$ is a confidence parameter whose value is set by the user, and $s_N^\star = |\mathcal{S}|$ is the number of support constraints for the optimal solution of the scenario program (19).

Proof. See proof for Theorems 2 and 4 in [67]. The proof are given for the case of optimization over Euclidean spaces and applies *mutatis mutandis* to the present more general setup presented to solve RBDO problems where λ is introduced.

The means to evaluate the bounds of the violation probability in (21) are given below. The set of support constraints $\mathcal{S}$ accounts for violated constraints, $\zeta^{\star(i)} > \lambda$, and active constraints, $w(\mathbf{d}^\star, \mathbf{x}^{(i)}) = \lambda$, so follows:

$$\mathcal{S} = \left\{ \mathbf{x} \in \mathcal{D}_N : w(\mathbf{d}^\star, \mathbf{x}) \geq \lambda \right\}, \tag{22}$$

For $\lambda = 0$ the violation probability $V(\mathbf{d}^\star)$ coincides with the true failure probability $P_f(\mathbf{d}^\star)$ which is unknown because the data-generating mechanism from which the scenarios were drawn is also unknown. The true probability $f_{\mathbf{x}}$ can be only known asymptotically when an infinite number of scenarios are collected, and this is never the case in practice.

Theorem 1 for $\lambda = 0$ provides bounds on the true failure probability, given by

$$P_f(\mathbf{d}^\star) \in \left[\underline{\epsilon}(s_N^\star), \overline{\epsilon}(s_N^\star)\right],$$

and, equivalently, on the prospective-reliability as follows:

$$R(\mathbf{d}^\star) \in \left[1 - \overline{\epsilon}(s_N^\star), 1 - \underline{\epsilon}(s_N^\star)\right],$$

where $\underline{\epsilon}(k) = \max\{0, 1 - \overline{t}(k)\}$, $\overline{\epsilon}(k) = 1 - \underline{t}(k)$ and $[\underline{t}, \overline{t}]$ are the two solutions a polynomial equation in t (see Theorem 4 in [67]):

$$\mathfrak{B}_N(t; k) - \frac{\beta}{2N} \sum_{i=k}^{N-1} \mathfrak{B}_i(t; k) - \frac{\beta}{6N} \sum_{i=N+1}^{4N} \mathfrak{B}_i(t; k) = 0, \tag{23}$$

where $\mathfrak{B}_N(t; k) = \binom{N}{k} t^{N-k}$ is the binomial expansion. Eq. (23) has two zeros when $k = 0, 1, \dots, N-1$. For a case $k = N$, consider the following polynomial equation in t:

$$1 - \frac{\beta}{6N} \sum_{i=N+1}^{4N} \mathcal{B}_i(t; k) = 0, \tag{24}$$

Eq. (24) admit one solution, which is $\overline{t}(N)$. The corresponding lower bound in this case is zero. As such, the prospective range of failure probabilities is $[\max\{0, 1 - \overline{t}(N)\}, 1]$.

The bounds $[\underline{\epsilon}, \overline{\epsilon}]$ are applicable to any convex scenario program, for any value of N, and the width of the interval quantifies the lack of data uncertainty affecting $d^\star$. Fig. 3 displays the prospective bounds on $V(\mathbf{d}^\star)$ computed for $\beta = 10^{-8}$ and for an increasing number of scenarios and support constraints. For a fixed N and β the bounds $[\underline{\epsilon}, \overline{\epsilon}]$ are both strictly increasing with the solution's complexity $s_N^\star$. Furthermore, notice that the width of the bounding interval decreases as N increases. This is due to the lower lack of data uncertainty associated with a decision taken using a large data set. For instance, consider a data set of very small size N and a scenario solution for which $s_N^\star = N$. The prospective-reliability bounds on $R(\mathbf{d}^\star)$ will result close to a vacuous interval [0,1]. In contrast, for $N \to \infty$ and $s_N^\star = N$, the lower bounds on the reliability $R(\mathbf{d}^\star)$ will converge to 1. Differently, when $N \to \infty$ and $s_N^\star = 0$ the upper bound on the reliability converge to 0. More in general, by increasing the available scenarios the width of the interval will progressively decrease and converge to the true reliability value given by the ratio $\lim_{N\to\infty} \frac{s_N^\star}{N}$

Table 1
Description of the proposed algebraic test cases adapted form [1,19,77], the baseline designs, the lower and upper bounds and the DGMs.

	Case 1 [77]	Case 2 [19]	Case 3 [1]
DGM	$x_1 : \mathcal{N}(0,1)$ $x_2 : \mathcal{N}(0,2)$	$x_1, x_2 : \mathcal{N}(0,1.2)$ $\Sigma_{1,2} = -0.9$	$x_1 : \mathcal{N}(0,1)$ $x_2 : \mathcal{N}(0,2)$
$\mathbf{x} \in$	$\mathbb{R}^2$	$\mathbb{R}^2$	$\mathbb{R}^2$
$g_1 =$	$-d_1 + x_1 + 5d_2x_2 - 2d_3(x_1 - x_2)^2$	$-d_1 - d_2^4(x_1 - x_2)^4 + \frac{(x_1 - x_2)}{\sqrt{2}}$	$\frac{x_2}{d_1} + \frac{x_1}{d_2} - d_3$
$g_2 =$	$-d_1(1 - x_2) + d_2x_1^2 - d_3x_1^3$	$-d_1 - d_2^4(x_1 - x_2)^4 - \frac{(x_1 - x_2)}{\sqrt{2}}$	$d_1x_1 - \frac{x_2}{d_2} - d_3$
$g_3 =$	–	$-d_3(d_4x_1 - x_2) - \frac{5.682d_2}{\sqrt{2}} - 2.2$	–
$g_4 =$	–	$-d_3(x_2 - d_4x_1) - \frac{5.682d_2}{\sqrt{2}} - 2.2$	–
$g \in$	$\mathbb{R}^2$	$\mathbb{R}^4$	$\mathbb{R}^2$
$\mathbf{d}_{bl}$	[2.5, 0.2, 0.06]	[0.2, 0.8801, 1, 6]	[1, 1, 1]
L_b	[0.5,–2,–0.3]	[–0.5, 0.1, 1, 5]	[0.5, 0.5, 0.5]
U_b	[4, 2, 0.3]	[0.5, 2, 2, 7]	[2, 2, 2]
$d \in$	$\mathbb{R}^3$	$\mathbb{R}^4$	$\mathbb{R}^3$

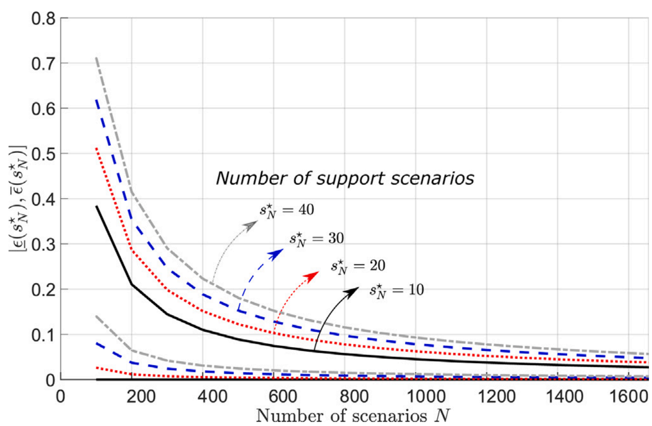

Fig. 3. The bounds $[\underline{\epsilon}, \overline{\epsilon}]$ computed for different N, $s_N^\star$ and for a confidence $\beta = 10^{-8}$.

The violation probability of individual requirements incurred by the solution to (19) or (20) is studied next. In this case we have:

$$V_j(\mathbf{d}^\star) = \mathbb{P}[g_j(\mathbf{d}^\star, \mathbf{x}) \geq \lambda_j] \tag{25}$$

Notice that V_j coincides with the true (but unavailable) failure probability for requirement j when $\lambda_j = 0$. A certificate of prospective-reliability is obtained for V via Eqs. (23) and (24):

$$V_j(\mathbf{d}^\star) \in [\underline{\epsilon}(v^\star_{N,j}), \overline{\epsilon}(v^\star_{N,j})]$$

where $v^\star_{N,j}$ is the number of support constraints for requirement j contained in the support set

$$\mathcal{S}_j = \left\{ \mathbf{x} \in \mathcal{D}_N : g_j(\mathbf{d}^\star, \mathbf{x}) \geq \lambda_j \right\}$$

The scenarios in $\mathcal{S}_j$ define constraints for requirement j is violated, for instance, the scenarios for which $\mathbf{x} \in \mathcal{F}_j(\mathbf{d}^\star)$ given a $\lambda_j = 0$. A scenario in $\mathcal{S}_j$ gives a contribution $\zeta_j^{(i)} > 0$ to the objective function in program (20) and, if removed, inevitably improves the objective function. Note that if a VaR level is selected such that $\lambda = \lambda_j$ for all $j = 1, \ldots, n_g$, then the sum of individual violation probabilities is $\sum_{j=1}^{n_g} V_j \geq V$ and $\sum_{j=1}^{n_g} v^\star_{N,j} \geq s_N^\star$. In other words, the probability of the event $w \geq \lambda$ is equal to the (union) probability of the events $g_j \geq \lambda$ minus the (intersection) probability of multiple failures. The equality sign holds if none of the scenarios fall in the intersection between failure regions, or if the individual failure regions are disjoint. If a VaR level is selected such that $\lambda \leq \min_{j=1,\ldots,n_g} \lambda_j$, the joint violation probability is $V \geq V_j$ for all j. In fact, if a random $\mathbf{x}$ leads to a failure event $g_j \geq \lambda_j$, then also the joint failure $w \geq \lambda$ occurs. The interested reader is reminded to [75] for further discussions on an extended version of convex scenario approaches with multiple chance constraints and sets of support constraints.

5. Case studies

The proposed approaches are tested on three RBDO problems having multiple, competitive, algebraic performance functions. Table 1 presents the reliability functions, the dimensionality of the problems, the baseline designs $\mathbf{d}_{bl}$, the lower and upper bounds on the design space and the Data-Generating Mechanisms (DGM). For these simple examples a low dimensional uncertainty space is selected to ease the visualization of the results, however, for scenario programs the dimension $n_{\mathbf{x}}$ is inconsequential [66]. Notice that the reliability functions are convex functions in d but not in $\mathbf{x}$. The optimization problem seeks a reliable designs $\mathbf{d}^\star$ constrained in $[L_b, U_b]$ so that a convex cost function $J(\mathbf{d}) = \sum_{i=1}^{n_d}(d_i + d_i^2)$ is minimized. The MATLAB's *fmincon* optimizer and the *'sqp'* algorithm are the numerical tools used to solve the problem. The baseline designs are arbitrarily selected for comparison and used as initial guesses for the solver.

For each test case we consider two sets of scenarios, $\mathcal{D}_{10^3}$ and $\mathcal{D}_{10^6}$, obtained from the stationary DGMs. The set with $N = 10^3$ is the only one used for the optimization routines. This represent real-life problems where only a limited number of data points is available to tackle optimization tasks. Differently, the set with $N = 10^6$ scenarios is considered unavailable for the optimization and only used to validate the prospective bounds $[\underline{\epsilon}, \overline{\epsilon}]$, introduced in Section 4.3. This is done by estimating the 'true' $V(\mathbf{d}^\star)$ and $V_j(\mathbf{d}^\star)$ with high accuracy which must lay with the prospective bounds with high confidence β and independently from the stationary probability $\mathbb{P}$ generating the data.

5.1. Results for CVaR constrained program (14)

The CVaR constrained optimization in Eq. (14) is used to solve the RBDO problems. A level $\alpha = 0.85$ is selected to constrain the probability of failure to the acceptable level $P_f < 0.15$. A Gaussian mixture model with five normal densities is fitted to $\mathcal{D}_{10^3}$ and used to estimate the CVaR constraint on w. Table 2 compares the reliability performances of the baseline design, $\mathbf{d}_{bl}$, and the optimized $\mathbf{d}^\circ$ resulting from the CVaR constrained program. The design cost J, the failure probability and the risk of extremes measured by the $CVaR_{0.95}(w)$ are presented as figures of merit. The CVaR constrained program yields designs that, compared to the baseline, are generally cheaper, more reliable and are characterized by a lower risk of facing extreme failures.

Table 2
Comparison between the reliability-costs of $\mathbf{d}_{bl}$, and the optimal designs $\mathbf{d}^{\circ}$ and $\mathbf{d}^{\star}$ resulting from programs (14) and (19), respectively.

Performance	Case 1			Case 2			Case 3		
Design program	$\mathbf{d}_{bl}$ –	$\mathbf{d}^{\circ}$ (14)	$\mathbf{d}^{\star}$ (19)	$\mathbf{d}_{bl}$ –	$\mathbf{d}^{\circ}$ (14)	$\mathbf{d}^{\star}$ (19)	$\mathbf{d}_{bl}$ –	$\mathbf{d}^{\circ}$ (14)	$\mathbf{d}^{\star}$ (19)
J	9.05	0.72	0.82	45.9	37.8	38.1	6	12.78	15.38
$CVaR_{0.95}(w)$	8.82	1.64	1.85	12.1	5.0	5.0	4.34	2.31	2.01
$\hat{P}_f$	0.337	0.606	0.423	0.67	0.28	0.10	0.61	0.234	0.186

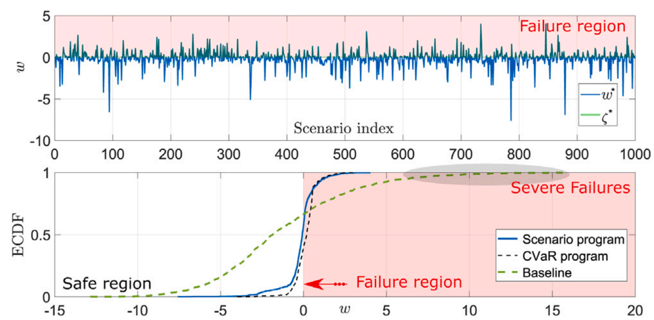

Fig. 4. The top panel: The worst-case performance $w(\mathbf{d}^{\star}, \mathbf{x})$, solid blue line, and $\zeta^{\star}$, green line, from $\mathcal{D}_{10^3}$. The bottom panel: A comparison between empirical CDFs with the results of program (19).

For instance consider Case 1, the optimized $\mathbf{d}^{\circ}$ results substantially cheaper compared to the baseline, from 9.05 to 0.72, and shows an overall mitigation of the risk, from $CVaR_{0.95}(w) = 8.2$ to only 1.64. However, the optimizer was unable to find a design with the required reliability level $P_f < 0.15$. This is due to the over-conservativism induced by a hard constraint on the conditional value-at-risk which led to an empty set of feasible design $\Theta^{CV}_{\alpha=0.85}$, i.e., designs that satisfy the constraint $CVaR_{0.85} \leq 0$.

5.2. Results for $\lambda = 0$

Program (19) with $\lambda = 0$ is used to amend for the deficiencies of program (14). A violation of a scenario constraints occurs when $\zeta^{(i)} > 0$, that is, the ith scenario fails to comply with at least one of the reliability requirements g_j. A high violation cost $\rho = 100$ is selected to maximize the reliability of the design. Fig. 4 presents the optimized vector of slack variables $\boldsymbol{\zeta}^{\star}$ (green solid line) and $w(\mathbf{d}^{\star}, \mathbf{x}^{(i)})$ (blue solid line) for the scenarios $\mathbf{x}^{(i)} \in \mathcal{D}_{10^3}$ and in correspondence of the optimum design $\mathbf{d}^{\star}$. The empirical CDF of $w(\mathbf{d}^{\star}, \mathbf{x}^{(i)})$ is presented in the bottom panel and compared to the result of the CVaR program (dashed line) and the baseline design (dotted line). It can be observed that for each $\zeta^{(i)} > 0$ the corresponding reliability violation is $w(\mathbf{d}, \mathbf{x}^{(i)}) = \zeta^{(i)}$ and thus, as expected, the proposed method minimizes a combination of $J(\mathbf{d})$ and the integral of w in the failure region expressed as a sum of $\zeta^{(i)}$. Table 4 presents the reliability performances of the designs $\mathbf{d}^{\star}$ obtained via the proposed scenario program. The designs $\mathbf{d}^{\star}$ result slightly more costly but for a gain in reliability when compared to program (14), and greatly improves the reliability compared to $\mathbf{d}_{bl}$. Most importantly, the proposed scenario program for RBDO always has a feasible solution. Furthermore, a certificate of prospective-reliability can be obtained for $\mathbf{d}^{\star}$.

Table 3 presents the results of the prospective-reliability analysis for $\mathbf{d}^{\star}$, that is, a certificate of robustness against future (yet unseen) scenarios. The prospective-reliability of $\mathbf{d}^{\star}$ depends on the number of active and violated constraints, see Eq. (21), which results $s^{\star}_{10^3} = 105$ for Case 2. For a confidence parameter $\beta = 10^{-8}$ (almost certainty) this leads to a prospective-reliability interval $R(\mathbf{d}^{\star}) \in [0.821, 0.9468]$ and to a range of prospective failure probabilities $P_f(\mathbf{d}^{\star}) \in [\underline{\epsilon}, \overline{\epsilon}]$. This is a powerful result which assures that the 'true' failure probability will

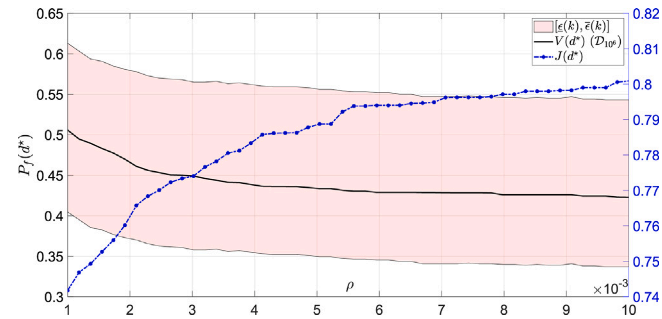

Fig. 5. Trade-off between cost $J(\mathbf{d}^{\star})$ and prospective-reliability bounds $[\underline{\epsilon}, \overline{\epsilon}]$ for Case 1.

result at worst 0.1788 and not better than 0.0532, hence informing the analyst on the robustness of $\mathbf{d}^{\star}$ against the uncertainty affecting the DGM (due limited availability of data). An accurate estimator of the violation probability $V(\mathbf{d}^{\star})$ is obtained using the set $\mathcal{D}_{10^6}$, which coincides with $P_f(\mathbf{d}^{\star})$ for $\lambda = 0$, and results contained within the bounds prescribed by scenario theory.

The prospective bounds are analogously obtained for the individual requirements and verified using the set $\mathcal{D}_{10^6}$ for all the other case studies leading to similar results. As example consider Case 1, the total number of support scenarios results $s^{\star}_{10^3} = 423$ leading to a prospective bound $V(\mathbf{d}^{\star}) \in [0.322, 0.527]$, which includes the 'true' failure probability $V(\mathbf{d}^{\star}) = 0.3995$. Concerning the individual requirements, the estimators of the true failure probability are 0.117 and 0.282 for requirement one and two, respectively. Both lay within the prospective ranges $[\underline{\epsilon}_1, \overline{\epsilon}_1] = [0.069, 0.206]$ and $[\underline{\epsilon}_2, \overline{\epsilon}_2] = [0.207, 0.396]$ obtained for 127 and $v^{\star}_{N,2}$ support scenarios, respectively. Notice that the prospective bounds always result $\overline{\epsilon}(s^{\star}_N) \leq \sum_{j=1}^{n_g} \overline{\epsilon}(v^{\star}_{N,j})$ and $\underline{\epsilon}(s^{\star}_N) \geq \sum_{j=1}^{n_g} \underline{\epsilon}(v^{\star}_{N,j})$.

5.3. Cost-reliability trade-off and ρ selection

Selecting a suitable value for the violation cost ρ can be challenging as it is difficult to forecast its impact on the design's failure probability. The designers might want to solve program (19) for different values of ρ and obtain a set of designs which compromise between costs $J(\mathbf{d}^{\star})$ and failure probability bounds according to Eq. (23). Fig. 5 presents the resulting trade-off between design's robustness (the reliability-bounds, red area) and its cost (blue dashed line). The figure is obtained for 50 distinct values of ρ, a confidence parameter $\beta = 10^{-8}$ and for case study 1 with $\lambda = 0$. Since the bounds are obtained by a repeated application of Eq. (23), the confidence that $\underline{\epsilon}(s^{\star}_{10^3}) \leq V(\mathbf{d}^{\star}) \leq \overline{\epsilon}(s^{\star}_{10^3})$ for all 50 values is 1–50 $\cdot\, \beta$, [67].

The numerical results for six values of ρ are presented in Table 4. The design's costs, the number of support scenarios $s^{\star}_N$ (samples in the failure region), and the prospective-reliability bounds are compared. As an example focus on Case 3. The designer might want to select a ρ which leads to a compromise reliability bounded in [0.3,0.5] and a cost $J(\mathbf{d}^{\star}) = 8.89$. Alternatively, an higher cost of $J(\mathbf{d}^{\star}) = 15.1$ for an improved reliability $P_f(\mathbf{d}^{\star}) \in [0.11, 0.28]$ might be the most suitable choice.

5.3.1. Results for $\lambda \neq 0$ and increasing N

Scenario program in Eq. (19) is tested on Case 3 for six values of $\lambda \in [-1.5, +1.5]$ and for six values of $N \in [50, 5000]$. Fig. 6 summarize the results of the analysis where the x-axis display the values of λ and the y-axis the probability of violation. The prospective range of violation probabilities for the joint requirement $w(\mathbf{d}, \mathbf{x}) < \lambda$ are displayed in the top panel whilst individual requirements $g_j(\mathbf{d}, \mathbf{x}) < \lambda$ are presented in the bottom panels. It can be observed that small λ values lead to wider scenario bounds on $\mathbb{P}[w(\mathbf{d}^{\star}, \mathbf{x}) \geq \lambda]$. For instance $\lambda = -1.5$ leads to a (random) number of support constraints $s^{\star}_{10^3} = 639$, which leads

Table 3
Prospective-reliability bounds and 'true' reliability for all requirements and individual requirements estimated with $\mathcal{D}_{10^6}$. Results for the optimized $\mathbf{d}^\star$ solutions of program (19) with $\lambda = 0$.

Robustness	All requirements		
$\beta = 10^{-8}$	Case 1	Case 2	Case 3
$s^\star_{10^3}$	423	105	186
R	0.6005	0.892	0.788
$[1-\overline{\epsilon}, 1-\underline{\epsilon}]$	[0.473, 0.678]	[0.821, 0.9468]	[0.725, 0.885]
Robustness	Individual requirements		
$\beta = 10^{-8}$	Case 1	Case 2	Case 3
$v^\star_{10^3,j}$	[127, 296]	[0, 1, 56, 48]	[81, 108]
$P_{f,1} \in [\underline{\epsilon}_1, \overline{\epsilon}_1]$	0.117 ∈ [0.069, 0.206]	0.001 ∈ [0, 0.022]	0.093 ∈ [0.037,0.148]
$P_{f,2} \in [\underline{\epsilon}_2, \overline{\epsilon}_2]$	0.282 ∈ [0.207, 0.396]	0.001 ∈ [0, 0.025]	0.123 ∈ [0.055,0.183]
$P_{f,3} \in [\underline{\epsilon}_3, \overline{\epsilon}_3]$	–	0.053 ∈ [0.021, 0.116]	–
$P_{f,4} \in [\underline{\epsilon}_4, \overline{\epsilon}_4]$	–	0.048 ∈ [0.016, 0.104]	–

Table 4
Trade-off between the prospective-reliability bounds and cost of the design $\mathbf{d}^\star$ for six values of the cost parameter ρ.

Cost-reliability	Case 1			Case 2			Case 3		
trade-off	J	$s^\star_{10^3}$	$[\underline{\epsilon}, \overline{\epsilon}]$	J	$s^\star_{10^3}$	$[\underline{\epsilon}, \overline{\epsilon}]$	J	$s^\star_{10^3}$	$[\underline{\epsilon}, \overline{\epsilon}]$
$\rho = 0.001$	0.742	510	[0.40,0.61]	33.7	719	[0.61,0.80]	2.74	819	[0.72,0.89]
$\rho = 0.01$	0.800	439	[0.33,0.54]	37.5	227	[0.14,0.32]	8.89	405	[0.30,0.50]
$\rho = 0.05$	0.819	425	[0.32,0.53]	38.1	129	[0.07,0.21]	13.7	209	[0.13,0.30]
$\rho = 0.1$	0.819	425	[0.32,0.53]	38.1	117	[0.06,0.19]	15.1	191	[0.11,0.28]
$\rho = 0.5$	0.823	423	[0.32,0.53]	38.1	107	[0.05,0.18]	15.3	187	[0.11,0.27]
$\rho = 1$	0.823	423	[0.32,0.52]	38.1	106	[0.05,0.18]	15.3	187	[0.11,0.27]

to a certificate $\mathbb{P}[w(\mathbf{d}^\star, \mathbf{x}) \geq -1.5] \in [0.533, 0.734]$. In contrast, the number of support constraints for $\lambda = 1.5$ is only $s^\star_{10^3} = 40$ and, thus, a tighter prospective certificate $\mathbb{P}[w(\mathbf{d}^\star, \mathbf{x}) \geq 1.5] \in [0.0122, 0.0932]$ can be obtained. In other words, no more than 9.32% of the unobserved scenarios will result in a worst-case performance $w \geq 1.5$ in correspondence of the design $\mathbf{d}^\star$ optimized with $\lambda = 1.5$. Intuitively, the tighter bounds on $\lambda = 1.5$ are due to the weaker statement on the tails of w. Differently, the probabilistic statement $\mathbb{P}[w(\mathbf{d}^\star, \mathbf{x}) \geq -1.5]$ is 'stronger' as it is made on a wider portion of the tail of w. However, it is also less guaranteed and results in wider prospective bounds. A similar trend can be observed for the violation probabilities $V_1(\mathbf{d}^\star)$ and $V_2(\mathbf{d}^\star)$ for the individual requirements. To check the validity of the scenario bounds, the 'true' violation probability $\mathbb{P}[w(\mathbf{d}^\star, \mathbf{x}) \geq \lambda]$ is estimated over the larger set of scenarios $\mathcal{D}_{10^6}$. The estimators of the true violation probability are displayed in Fig. 6 by red marked lines and, for any λ, it results within the bounds prescribed by scenario theory.

The prospective ranges $[\overline{\epsilon}(s^\star_N), \overline{\epsilon}(s^\star_N)]$ for different sample sizes N are displayed by the blue areas in Fig. 6 where a lighter color indicates a lower availability of samples N. As expected, the bounds get tighter for higher N and always include the violation probability estimate (red marked lines). Tighter bounds are due to the increasing knowledge on the underlying $\mathbb{P}$ generating the data. Finally, note that the prospective ranges of violation probabilities coincides with the ranges of failure probabilities for $\lambda = 0$. In general, these bounds might be slightly different from the one obtained in Section 5.2 since $s^\star_N$ is a random number which depends on the available $\mathcal{D}_N$.

5.4. Trade reliability of individual requirements program (20)

In some cases, only a subset of reliability requirements is considered of vital importance for the health state of a system whilst other requirements are considered less relevant. It is therefore of practical interest to prescribe design solutions that reliability well-reflects these different weights. To this end, we test scenario optimization program (20) with individual soft constraints to solve Case 3. For the sake of this analysis, we assume an expert considers the second reliability requirement (g_2) to be less stringent than requirement one (g_1). Further, we assume that the designer wishes to prescribe a $\mathbf{d}^\star$ having individual failure probabilities which are at least $P_{f,1} < 0.2$ and $P_{f,2} < 0.5$ and a budget constraint $J < 10$ is also imposed on the design. A set of design solutions $\mathbf{d}^\star$ is obtained using program (20) for a grid of equally spaced (ρ_1, ρ_2) and for a scenario set of size $N = 200$. The result is a set of trade-off designs, which compromise between the minimization of $J(\mathbf{d})$ and the total cost of violations for the individual reliability requirements, i.e., $\rho_j \sum_{i=1}^{N} \zeta_j^{(i)}$.

Fig. 7 summarizes the result of this analysis. The set of pairs (ρ_1, ρ_2) which led to feasible designs in accordance with the requirements $P_{f,1}(\mathbf{d}^\star) < 0.2$, $P_{f,2}(\mathbf{d}^\star) < 0.5$, and $J(\mathbf{d}^\star) < 10$ is highlighted in red. Four values of (ρ_1, ρ_2) are selected (highlighted by black arrows) and the resulting designs have the lowest costs, the lowest individual failure probabilities for the requirements one and two, and a compromise solution, respectively. Table 5 presents their costs and prospective-reliability scores. The solution having lowest P_f coincides with the design minimizing $P_{f,2}$. As expected, higher values of ρ_1 (ρ_2) lead to better reliability performance for the first (second) reliability requirement. For instance, the design with the lowest $P_{f,1}$ results in $\hat{P}_{f,1} = 30/200 \in [\underline{\epsilon}_1, \overline{\epsilon}_1]$, $\hat{P}_{f,2} = 46/200 \in [\underline{\epsilon}_2, \overline{\epsilon}_2]$ for the individual requirements estimates, $\hat{P}_f = 72/200 \in [\underline{\epsilon}, \overline{\epsilon}]$ for the overall failure probability, and in a cost of 9.95 monetary units. Differently, the most economical solutions only cost 7.85 but, in turn, it is inferior in terms of reliability performance, e.g., $\hat{P}_f = 94/200$. Because of the competitiveness between overall reliability and cost, as well as between individual reliability requirements, the set of pairs (ρ_1, ρ_2) highlighted in red defines a 3-dimensional Pareto's front in the space of $P_{f,1}$, $P_{f,2}$ and J.

6. Testing on two real-world examples

We apply the proposed method to optimize the cost and expected severity of two realistic engineering examples. In the first problem, we optimize the design of an aircraft lateral motion controller. This problem includes 13 uncertain variables and 16 design parameters. In the second examples, we optimize the design of a 72-bar multi-story space truss and the problem includes 78 uncertain factors and 18 design parameters. This last example has a relatively large number of design parameters and uncertain factors. It is used to demonstrate the scalability of the proposed method to realistic engineering problems for which only a black-box computational model of the system and experimental data about uncertain material proprieties are available.

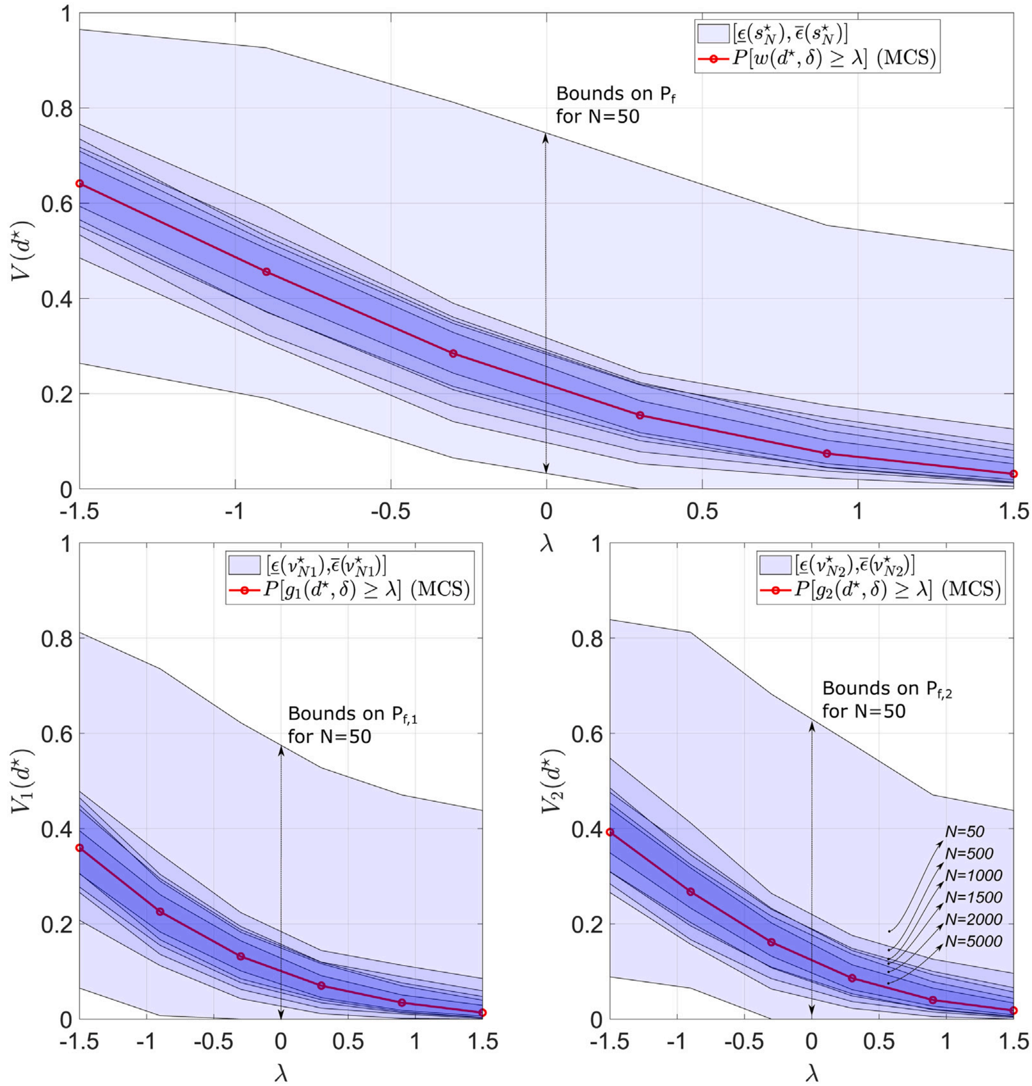

Fig. 6. Prospective-reliability bounds on $V(\mathbf{d}^\star)$ and individual $V_j(\mathbf{d}^\star)$ for six sizes N and $\lambda \in [-1.5, +1.5]$. The 'true' violation probability approximated via the set $\mathcal{D}_{10^6}$ is displayed by red marked lines.

Table 5
The performance of the designs, of program (20), leading to the best reliability, the best cost and a compromise between the two. Solution are selected among the one fulfilling the conditions $P_{f,1}(\mathbf{d}^\star) < 0.2$, $P_{f,2}(\mathbf{d}^\star) < 0.5$ and $J(\mathbf{d}^\star) < 10$.

	$s^\star_{200}$	$v^\star_{200,1}$	$v^\star_{200,2}$	$J(\mathbf{d}^\star)$	$[\underline{\epsilon}, \overline{\epsilon}]$	$[\underline{\epsilon}_1, \overline{\epsilon}_1]$	$[\underline{\epsilon}_2, \overline{\epsilon}_2]$
Best P_f and $P_{f,1}$	72	30	46	9.957	[0.169,0.588]	[0.0375,0.3536]	[0.0821,0.4498]
Best cost J	94	39	60	7.857	[0.255,0.692]	[0.0618,0.4090]	[0.1270,0.5265]
Best $P_{f,2}$	64	37	28	9.967	[0.141,0.547]	[0.0563,0.3971]	[0.0322,0.3408]
Compromise	81	35	49	9.143	[0.203,0.632]	[0.0508,0.3849]	[0.0913,0.4667]

6.1. Design of an aircraft lateral motion controller

The soft-constrained RBDO program, proposed in Eq. (19), is used to optimize the reliability of an aircraft lateral motion controller. The dynamics of the system is defined by the following state–space model [78]:

$$\dot{\mathbf{s}}(t) = \mathbf{A}(\mathbf{x})\mathbf{s}(t) + \mathbf{B}(\mathbf{x})\mathbf{u}(t), \tag{26}$$

where $\mathbf{u}(t) \in \mathbb{R}^2$, is the controller input vector defining the rudder and aileron deflections and $\mathbf{s}(t) \in \mathbb{R}^4$, is a state vector representing the aircraft blank angle and its derivative, the sideslip angle, the yaw rate. The matrices $\mathbf{A}$ and $\mathbf{B}$ in Eq. (26) are determined from a vector $\mathbf{x}$ containing $n_x = 13$ uncertain aircraft motion parameters. The elements of the aircraft state matrices are given by:

$$A(\mathbf{x}) = \begin{pmatrix} 0 & 1 & 0 & 0 \\ 0 & L_p & L_\beta & L_r \\ g/V & 0 & Y_\beta & -1 \\ N_{\dot\beta}(g/V) & N_p & N_\beta + N_{\dot\beta} Y_\beta & N_r - N_{\dot\beta} \end{pmatrix},$$

$$B(\mathbf{x}) = \begin{pmatrix} 0 & 0 \\ 0 & L_{\delta_a} \\ Y_{\delta_r} & 0 \\ N_{\delta_r} + N_{\dot\beta} Y_{\delta_r} & N_{\delta_a} \end{pmatrix}.$$

Table 6 presents the mean value for the uncertain parameters $\mathbf{x}$.

The goal of this problem is to identify a reliable state feedback controller that stabilizes the system by achieving a target decay rate

Table 6
The 13 uncertain parameters affecting the aircraft motion [79] and their nominal values. Scenarios are generated from a normal distributions with mean $\mu_{\mathbf{x}}$ and cov 0.3.

$\mathbf{x}$	L_p	L_β	L_r	g/V	Y_β	$N_{\dot\beta}$	N_p	N_β	N_r	L_{δ_a}	Y_{δ_r}	N_{δ_r}	N_{δ_a}
$\mu_{\mathbf{x}}$	−2.93	−4.75	0.78	0.086	−0.11	0.1	−0.042	2.601	−0.29	−3.91	0.035	−2.5335	0.31

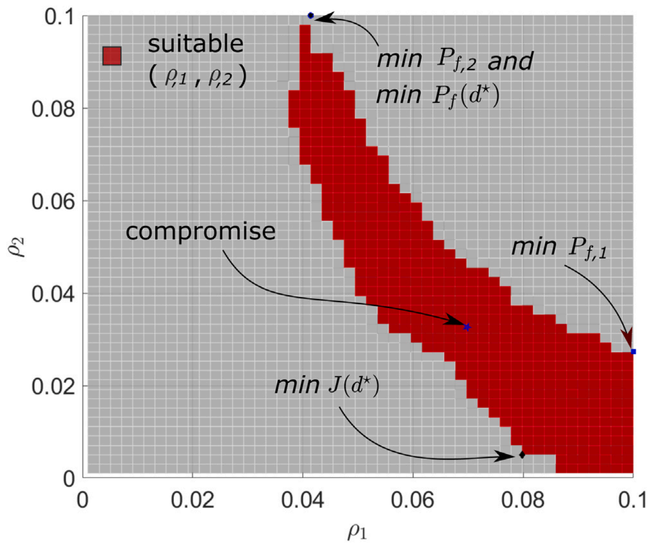

Fig. 7. The set of suitable (ρ_1, ρ_2) to achieve a $P_{f,1} < 0.2$, $P_{f,2} < 0.5$ and $J < 10$ for Case 3, the red area. Markers display the designs leading to minimum $P_f(\mathbf{d}^\star)$, $P_{f,1}(\mathbf{d}^\star)$, $P_{f,2}(\mathbf{d}^\star)$, and $J(\mathbf{d}^\star)$ within the set of suitable (ρ_1, ρ_2).

$\gamma > 0$. A decay rate $\gamma = 0.1$ is considered. A sufficient condition for the existence of such a controller requires finding a matrix $W(\mathbf{d}) \in \mathbb{R}^{4\times 2}$ and a symmetric positive definite matrix $P(\mathbf{d}) \in \mathbb{R}^{4\times 4}$ satisfying the following convex quadratic performance criterion:

$$\mathbf{g}(\mathbf{d},\mathbf{x}) = \mathbf{A}(\mathbf{x})\mathbf{P}(\mathbf{d}) + \mathbf{P}(\mathbf{d})\mathbf{A}^T(\mathbf{x})$$
$$+\mathbf{B}(\mathbf{x})\mathbf{W}^T(\mathbf{d}) + \mathbf{W}(\mathbf{d})\mathbf{B}^T(\mathbf{x}) + 2\gamma\mathbf{P}(\mathbf{d}) \preccurlyeq 0$$

where $\preccurlyeq$ denotes negative semi-definite matrices, $\mathbf{g} \in \mathbb{R}^{4\times 4}$ is a square matrix, and the elements of the matrices $\mathbf{P}(\mathbf{d})$ and $\mathbf{W}(\mathbf{d})$ are defined by a 18 dimensional design vector $\mathbf{d}$. A controller $\mathbf{d}$ that achieves the desired decay rate for a scenario $\mathbf{x}$ if

$$w(\mathbf{d},\mathbf{x}) = \Lambda_{max}[\mathbf{g}(\mathbf{d},\mathbf{x})] \le 0,$$

where $\Lambda_{max}[\cdot]$ denotes the maximum eigenvalue of $\mathbf{g}$.

A candidate design solution was proposed in the Ref. [79] as the result of a sequential design procedure. We adopt this design as the base line solution. By assuming the uncertain factors normally distributed with mean values given in Table 6 and coefficient of variation 0.3, the baseline design results in a high failure probability of $P_f = 0.54$. We now compare the baseline against a design obtained via the proposed soft-constrained scenario program in Eq. (19). We first assume $N = 300$ samples of $\mathbf{x}$ are available to optimize $\mathbf{d}$ via the following soft-constrained scenario RBDO program:

$$\min_{\mathbf{d},\zeta} Tr[\mathbf{P}] + \rho \sum_{i=1}^{N} \zeta^{(i)} :$$
$$s.t.\ \ \mathbf{P}(\mathbf{d}) \succcurlyeq \theta I$$
$$w(\mathbf{d},\mathbf{x}^{(i)}) \le \zeta^{(i)},\ i = 1,\dots,300$$
$$\zeta^{(i)} \ge 0,\ i = 1,\dots,300$$

where $Tr[\cdot]$ is the trace operator and θ is a small value ensuring positive definiteness of $\mathbf{P}(\mathbf{d})$. We select a high cost of violations to give more importance to a minimize the risk rather than the trace of the matrix. This yield an optimal design with zero violations and $s^\star_{300} = 0$. This means that the slack variables result $\zeta^{(i),\star} = 0$ for all $i = 1,\dots,300$ and the estimate of the failure probability results $\hat{P}_f(\mathbf{d}^\star) = 0$.

Theorem 1 is used to derive the following certificate of probabilistic performance for the optimize design:

$$\mathbb{P}^{300}[0 \le P_f(\mathbf{d}^\star) \le 0.038] \ge 1 - 10^{-4}$$

This certificate ensures a failure probability bounded in $[0, 0.038]$ with a high degree of confidence (the right-hand side of the equation). This ensures that the design $\mathbf{d}^\star$ will achieve the desired decay rate γ at least 96.2% of the times. This certificate of probabilistic performance holds independently from the true distribution of the uncertain data and is data-dependent because computed based on the availability of the 300 samples. We estimated the true probability of failure and it results in $P_f = 0.0087$. This verifies the validity of the upper and lower bounds and shows that the proposed soft-constrained program substantially improved the reliability of the controller.

6.2. Design of a 72-bar four level skeletal tower

In the next engineering example, the weight of 72 bar multi-story space truss structure must be minimized while ensuring a high-reliability performance. The problem was solved using deterministic optimization methods, see e.g. [80,81], however, deterministic approaches only focused on the minimization of the weight and not on the reliability. Differently, RBDO approaches have been proposed to minimize both the failure probability and weight, see e.g., [82,83]. None of the reviewed works proposed a reliability-based nor a risk-based design without prescribing a model for the uncertainty.

Fig. 8 presents the geometry of the structure. The 72 bars are categorized into 16 groups and the design vector $d = [A_1,\dots,A_{16}]$ defines the 16 cross-sectional areas to be minimized. The objective is to minimize the weight of the structure that is proportional to the structure's volume and its cost. The unit material density is 0.1 [lb/in.^{2}]. Reliability requirements are imposed on the displacement of the nodes and maximum tension and compression stresses. The maximum displacement for the nodes top four nodes is ± 0.25 [in.] for x, y and z directions, the maximum allowable stress for all members is ± 25 [ksi] (the same in tension and compression), the range of acceptable cross-sectional design areas varies from 0.1 [in.^{2}] to 4.0 [in.^{2}]. We combined the two load cases presented in [80] for a total of six loads components affecting the nodes 1 to 4. We consider the modulus of elasticity and the loads to be uncertain and only N samples of them are available to optimize the structure's weight and reliability. The samples of the 72 Young's modulus are drawn from a normal distribution with a mean 10^4 [ksi] and standard deviation of 10^2 [ksi]. The samples of the loads are obtained from normal distributions with mean −5 [kips] on the vertical z-component and +5 [kips] in the x and y directions [80]). A standard deviation of 0.5 [kips] is assumed for the loads. The modified version of this problem includes $n_x = 78$ random variables $n_d = 16$ design parameters, and $n_g = 84$ reliability requirements (72 on the maximum allowable stress and 12 maximum displacements).

Soft-constrained scenario solutions to this design problem is obtained using Eq. (19) and selecting a cost of violations $\rho = 10^5$ and for 3 number of sample $N = 100$, $N = 200$ and $N = 500$. We assume the system response can be only evaluated using a black-box model and assume convexity of the volume function and the reliability performance functions. Table 7 presents the designs resulting from the proposed soft-constrained scenario RBDO approach and compares their performance to four deterministic designs and three RBDO designs. As

Table 7
The cross sectional areas, weight and reliability performance of four deterministic designs, six RBDO designs (3 from literature and 3 proposed in this paper). See [82, Table 7] for more detailed description on the deterministic designs acronyms.

		Literature							This work		
Design		Deterministic				RBDO					
Area	Members	HSPO [82]	SAHS [84]	PSO [84]	TLBO [80]	C-[85]	E-[85]	aeDE [83]	(N = 100)	(N = 200)	(N = 500)
A_1	1–4	1.857	1.86	1.7427	1.906	3.18	3.199	11.49	3.408	3.7094	3.999
A_2	5–12	0.505	0.521	0.5185	0.506	1.48	1.486	2.88	0.833	0.912	0.8409
A_3	13–16	0.1	0.1	0.1	0.1	0.33	0.33	1.61	0.1	0.1	0.1
A_4	17–18	0.1	0.1	0.1	0.1	0.1	0.10	1.61	0.1	0.1	0.1
A_5	19–22	1.255	1.271	1.3079	1.262	2.6	3.2	7.2	2.467	2.69	1.804
A_6	23–30	0.503	0.509	0.5193	0.511	1.58	1.599	1.98	0.833	0.91	1.38
A_7	31–34	0.1	0.1	0.1	0.1	0.1	0.119	1.62	0.1	0.1	0.1
A_8	35–36	0.1	0.1	0.1	0.1	0.1	0.136	1.62	0.1	0.1	0.1
A_9	37–40	0.496	0.485	0.5142	0.532	1.61	1.70	1.62	1.45	1.62	2.074
A_{10}	41–48	0.506	0.501	0.5464	0.516	1.65	1.63	3.55	0.837	0.1	1.092
A_{11}	49–52	0.1	0.1	0.1	0.1	0.1	0.1	1.62	0.1	0.1	0.1
A_{12}	53–54	0.1	0.1	0.1095	0.1	0.1	0.1	1.62	0.1	0.1	0.12
A_{13}	55–58	0.1	0.168	0.1615	0.156	0.637	0.37	1.62	0.439	0.478	0.251
A_{14}	59–66	0.524	0.584	0.5092	0.549	1.581	1.606	1.62	0.852	0.935	0.782
A_{15}	67–70	0.4	0.433	0.4967	0.409	0.1	0.534	1.62	0.697	0.741	0.459
A_{16}	71–72	0.534	0.520	0.5619	0.569	0.116	0.802	1.62	0.892	0.928	0.823
Weight [lb]		369.65	380.6	381.9	379.6	913.47	972.8	1974	634.89	690.15	710.04
$\hat{P}_f$		1	1	1	1	0.017	0	0	0.02	0.005	0.006
$CVaR_{0.95}(w)$		1.18	0.76	0.77	0.77	−0.0017	−0.26	−0.60	−0.0189	−0.1119	−0.034
Function count		125 000	13 742	n.a.	19 709	n.a.	n.a.	993 600	10 885	21 064	25 333
$[\underline{\epsilon}, \overline{\epsilon}], \beta = 10^{-4}$		–	–	–	–	–	–	–	[0,0.164]	[0,0.074]	[0,0.0395]

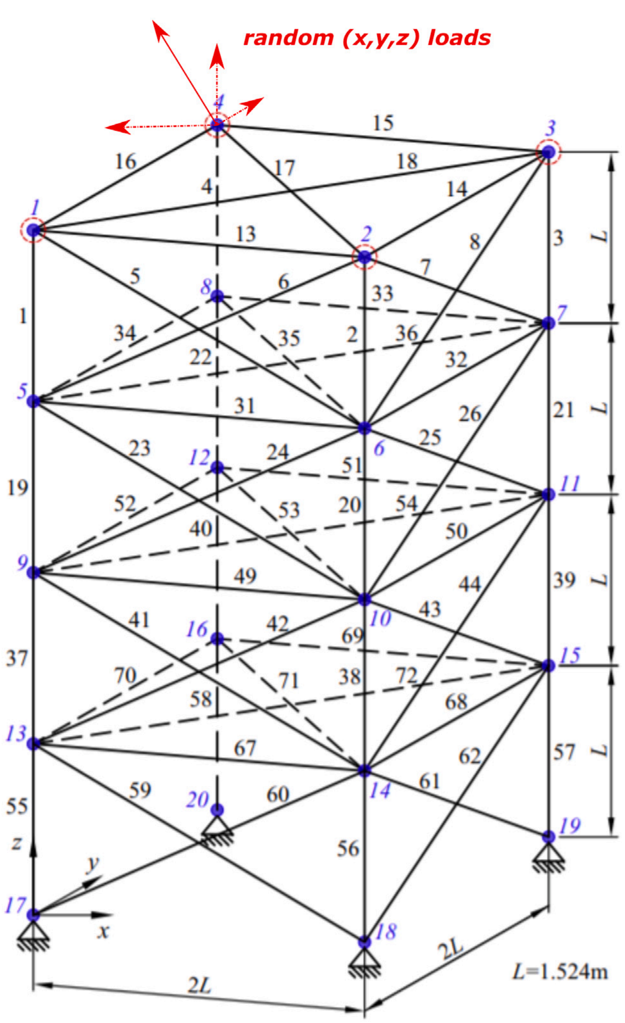

Fig. 8. The geometry of the low-weight 72-bar multi-story space truss.
Source: Figure adapted from [81]

a figure of merit, we present the resulting weight of the structure, its empirical failure probability, its risk measured by the conditional value-at-risk, $CVaR_{0.95}(w)$, and the computational cost of the optimization (expressed as an average number of function evaluations). Deterministic designs result in lower costs and are highly unreliable whilst reliability-based designs are reliable but expensive. In contrast with the reviewed results, the proposed soft-constrained design achieved a good compromise between cost and reliability and is equipped with an epistemic interval on its failure probability, see the last row of Table 7. This certificate guarantees a minimum probabilistic level of safety and reflects the availability of data when the design was introduced. If more samples are collected, a more informative and accurate reliability certificate can be prescribed. However, note that the number of available scenarios has a significant impact on the computational cost of the analysis and the manufacturing cost of the structure. This can be regarded as drawbacks of the proposed method and will be discussed in the next section.

6.3. Summary and discussion on the computational cost and limitations of the proposed method

We demonstrated the applicability of the proposed approach for risk- and reliability-based design on three easily reproducible analytical examples, and two realistic engineering problems. Table 7 compares the computational cost of our method (in function counts) with the cost of deterministic optimizers and RBDO procedures taken from literature. Note that the reliability function must be evaluated N times for each iteration of the soft-constrained method, one for each scenario constraint. Moreover, the relaxation terms ζ expand the design space with N additional dimensions. Hence, our method achieves a satisfactory numerical efficiency when a small number of scenario constraints are available. In this case, the number of function counts is comparable to deterministic optimization methods. Conversely, it may be difficult to apply the proposed approach when many samples are available, i.e., big data sets, and when the reliability function g is numerical costly to evaluate (such as a finite element code or CFD simulator). Note that reliability functions g are treated as black-box models in this work and convexity in the design space is assumed for the formal derivation of the reliability bounds. Hence, the high computational cost of the model g, its convexity in d, and the high dimensionality of the design space limit the applicability of the proposed approach. However, the dimensionality of the state–space defining g should not be regarded as a limiting factor. In facts, a reliability function defined by a large state–space can be relatively easy to compute, e.g., for quasi-static and linear models. In these cases, the scenario approach offers a very effective way of tackling RBDO problems.

A solution to these problems can be to replace the computationally expensive model g with a low-fidelity convex approximation of it, like a reduced-order model also known as an emulator. If the number of scenarios is very large, a subset of the data set containing the worst-case scenarios may be considered. However, the worst-case scenarios may change for different $\mathbf{d}$ and this would require periodically update the list of worst-case candidates while optimizing the design. These can be regarded as possible targets for a future research direction.

7. Conclusions

The approach proposed in [1], which is applicable to RBDO problems having reliability functions depending arbitrarily on d, yields a probabilistic certificate of performance for the optimal design. This certificate is an upper bound on the probability of the system exhibiting severe failures for future data. This paper extends the developments therein by providing tighter bounds when the RBDO program can be assumed convex. A new scenario program with soft constraints is proposed and the method can be used to identify reliable designs that minimize a weighted combination of system cost and risk without prescribing a model for the uncertainty. Without relaxing the constraints a scenario optimization program might not admit a solution. Multiple weighting factors have been proposed to control the importance of minimizing the cost over the risks of facing severe failure for different failure modes. Strong model assumptions are often needed to define probability distributions given insufficient data. As such, this practice might lead to RBDO and risk-based designs that significantly underperform in practice. Avoiding the prescription of a model for the uncertainty makes the resulting design exempt from the subjectivity induced by such a practice. Recent results from scenario theory are used in this work to prescribe bounds on the true reliability of a design and, in general, on the probability of the design facing failures of magnitudes exceeding a predefined value-at-risk threshold. These ranges of probabilities, called prospective-reliability bounds, hold independently of the underlying data-generating mechanism (for any probability distribution consistent with the data), non-asymptotically (for any number of samples N), and given mild assumptions on the uncertainty. This probabilistic certificate of performance offers a powerful robustness and safety monitoring tool which reveals the current state of knowledge and uncertainty. This is an invaluable tool for analysts which can be conveniently used to support better decision-making and prescribe designs for which reliability and robustness are certifiable.

Replication package: The data and scripts for the numerical analysis are publicly available at the GitHub repository: https://github.com/Roberock/ScenarioRBDO.

CRediT authorship contribution statement

Roberto Rocchetta: Conceptualization, Methodology, Software, Data curation, Visualization, Writing – original draft, Writing – review & editing. **Luis G. Crespo:** Supervision, Funding acquisition, Project administration, Writing – review & editing.

Declaration of competing interest

The authors declare that they have no known competing financial interests or personal relationships that could have appeared to influence the work reported in this paper.

Acknowledgments

The authors would like to acknowledge the gracious support of this work through the local authorities under grant agreement "ITEA-2018-17030-Daytime"

References

[1] Rocchetta R, Crespo LG, Kenny SP. A scenario optimization approach to reliability-based design. Reliab Eng Syst Saf 2020;196:106755.
[2] Zio E. Reliability engineering: Old problems and new challenges. Reliab Eng Syst Saf 2009;94(2):125–41.
[3] Coit DW, Zio E. The evolution of system reliability optimization. Reliab Eng Syst Saf 2019;192:106259.
[4] Enevoldsen I, Sørensen J. Reliability-based optimization in structural engineering. Struct Saf 1994;15(3):169–96.
[5] Rocchetta R, Patelli E. Stochastic analysis and reliability-cost optimization of distributed generators and air source heat pumps. In: 2nd international conference on system reliability and safety (ICSRS). 2017, p. 31–5. http://dx.doi.org/10.1109/ICSRS.2017.8272792.
[6] Yuan X, Lu Z. Efficient approach for reliability-based optimization based on weighted importance sampling approach. Reliab Eng Syst Saf 2014;132:107–14.
[7] Shan S, Wang GG. Reliable design space and complete single-loop reliability-based design optimization. Reliab Eng Syst Saf 2008;93(8):1218–30.
[8] Meng Z, Keshtegar B. Adaptive conjugate single-loop method for efficient reliability-based design and topology optimization. Comput Methods Appl Mech Engrg 2019;344:95–119.
[9] Wang Y, Hao P, Yang H, Wang B, Gao Q. A confidence-based reliability optimization with single loop strategy and second-order reliability method. Comput Methods Appl Mech Engrg 2020;372:113436.
[10] Yao W, Chen X, Huang Y, van Tooren M. An enhanced unified uncertainty analysis approach based on first order reliability method with single-level optimization. Reliab Eng Syst Saf 2013;116:28–37.
[11] Torii A, Lopez R, Miguel L. A second order SAP algorithm for risk and reliability based design optimization. Reliab Eng Syst Saf 2019;190:106499.
[12] Du X, Chen W. Sequential optimization and reliability assessment method for efficient probabilistic design. Proceedings of the ASME Design Engineering Technical Conference 2002;2:871–80.
[13] Li H-S, Au S-K. Design optimization using subset simulation algorithm. Struct Saf 2010;32(6):384–92, Modeling and Analysis of Rare and Imprecise Information.
[14] de Angelis M, Patelli E, Beer M. Advanced line sampling for efficient robust reliability analysis. Struct Saf 2015;52:170–82.
[15] Chaudhuri A, Kramer B, Willcox KE. Information reuse for importance sampling in reliability-based design optimization. Reliab Eng Syst Saf 2020;201:106853.
[16] Nikolaidis E, Burdisso R. Reliability based optimization: A safety index approach. Comput Struct 1988;28(6):781–8.
[17] Kuschel N, Rackwitz R. Two basic problems in reliability-based structural optimization. Math Methods Oper Res 1997;46(3):309–33.
[18] Cizelj L, Mavko B, Riesch-Oppermann H. Application of first and second order reliability methods in the safety assessment of cracked steam generator tubing. Nucl Eng Des 1994;359–68.
[19] Schuëller G, Pradlwarter H, Koutsourelakis P. A critical appraisal of reliability estimation procedures for high dimensions. Probab Eng Mech 2004;19(4):463–74.
[20] Li J, Xiu D. Evaluation of failure probability via surrogate models. J Comput Phys 2010;229(23):8966–80.
[21] Chen P, Quarteroni A. Accurate and efficient evaluation of failure probability for partial different equations with random input data. Comput Methods Appl Mech Engrg 2013;267:233–60.
[22] Peherstorfer B, Kramer B, Willcox K. Combining multiple surrogate models to accelerate failure probability estimation with expensive high-fidelity models. J Comput Phys 2017;341:61–75.
[23] Peherstorfer B, Kramer B, Willcox K. Multifidelity preconditioning of the cross-entropy method for rare event simulation and failure probability estimation. SIAM/ASA J Uncertain Quantif 2018;6(2):737–61.
[24] Dige N, Diwekar U. Efficient sampling algorithm for large-scale optimization under uncertainty problems. Comput Chem Eng 2018;115:431–54.
[25] Li M, Wang Z. Surrogate model uncertainty quantification for reliability-based design optimization. Reliab Eng Syst Saf 2019;192:106432.
[26] Ullmann E, Papaioannou I. Multilevel estimation of rare events. SIAM/ASA J Uncertain Quantif 2015;3:922–53.
[27] Charnes A, Cooper WW. Chance-constrained programming. Manage Sci 1959;6(1):73–9.
[28] Keshtegar B, Chakraborty S. Dynamical accelerated performance measure approach for efficient reliability-based design optimization with highly nonlinear probabilistic constraints. Reliab Eng Syst Saf 2018;178:69–83.
[29] Takeda A, Kanamori T. A robust approach based on conditional value-at-risk measure to statistical learning problems. European J Oper Res 2009;198(1):287–96.

[30] Mena R, Hennebel M, Li Y-F, Ruiz C, Zio E. A risk-based simulation and multi-objective optimization framework for the integration of distributed renewable generation and storage. Renew Sustain Energy Rev 2014;37:778–93.
[31] Rockafellar R, Royset J. On buffered failure probability in design and optimization of structures. Reliab Eng Syst Saf 2010;95(5):499–510.
[32] Crespo LG, Colbert BK, Kenny SP, Giesy DP. On the quantification of aleatory and epistemic uncertainty using sliced-normal distributions. Systems Control Lett 2019;134:104560.
[33] Rocchetta R, Broggi M, Patelli E. Do we have enough data? Robust reliability via uncertainty quantification. Appl Math Model 2018;54:710–21.
[34] Sarykalin S, Serraino G, Uryasev S. Value-at-risk vs. Conditional value-at-risk in risk management and optimization. In: State-of-the-art decision-making tools in the information-intensive age. Institute for Operations Research and the Management Sciences (INFORMS); 2014, p. 270–94.
[35] Lebrun R, Dutfoy A. An innovating analysis of the nataf transformation from the copula viewpoint. Probab Eng Mech 2009;24(3):312–20.
[36] Lebrun R, Dutfoy A. A generalization of the nataf transformation to distributions with elliptical copula. Probab Eng Mech 2009;24(2):172–8.
[37] Ben-Haim Y. A non-probabilistic concept of reliability. Struct Saf 1994;14(4):227–45.
[38] Meng Z, Zhang Z, Zhou H. A novel experimental data-driven exponential convex model for reliability assessment with uncertain-but-bounded parameters. Appl Math Model 2020;77:773–87.
[39] Shafer G. A mathematical theory of evidence turns 40. Internat J Approx Reason 2016;79:7–25.
[40] Ferson S, Kreinovich V, Ginzburg L, Myers DS, Sentz K. Constructing probability boxes and Dempster-Shafer structures, Vol. 835. Sandia National Laboratories; 2002.
[41] Dubois D, Prade H. Possibility theory, probability theory and multiple-valued logics: A clarification. Ann Math Artif Intell 2001;32:35–66. http://dx.doi.org/10.1023/A:1016740830286.
[42] Walley P. Statistical reasoning with imprecise probabilities. Chapman & Hall/CRC monographs on statistics & applied probability, Taylor & Francis; 1991.
[43] Zadeh L. Fuzzy sets. Inf Control 1965;8(3):338–53.
[44] Liu Z, Liu Y, Dezert J, Cuzzolin F. Evidence combination based on credal belief redistribution for pattern classification. IEEE Trans Fuzzy Syst 2020;28(4):618–31.
[45] Rocchetta R, Zio E, Patelli E. A power-flow emulator approach for resilience assessment of repairable power grids subject to weather-induced failures and data deficiency. Appl Energy 2018;210:339–50.
[46] Beer M, Ferson S, Kreinovich V. Imprecise probabilities in engineering analyses. Mech Syst Signal Process 2013;37(1–2):4–29.
[47] Eldred M, Swiler L, Tang G. Mixed aleatory-epistemic uncertainty quantification with stochastic expansions and optimization-based interval estimation. Reliab Eng Syst Saf 2011;96(9):1092–113, Quantification of Margins and Uncertainties.
[48] Xie W. On distributionally robust chance constrained programs with wasserstein distance. Math Program 2021;186:115–55.
[49] Nannapaneni S, Mahadevan S. Reliability analysis under epistemic uncertainty. Reliab Eng Syst Saf 2016;155:9–20.
[50] Meng Z, Pang Y, Pu Y, Wang X. New hybrid reliability-based topology optimization method combining fuzzy and probabilistic models for handling epistemic and aleatory uncertainties. Comput Methods Appl Mech Engrg 2020;363:112886.
[51] Wang L, Ma Y, Yang Y, Wang X. Structural design optimization based on hybrid time-variant reliability measure under non-probabilistic convex uncertainties. Appl Math Model 2019;69:330–54.
[52] Meng Z, Zhou H. New target performance approach for a super parametric convex model of non-probabilistic reliability-based design optimization. Comput Methods Appl Mech Engrg 2018;339:644–62.
[53] Wang L, Liu D, Yang Y, Wang X, Qiu Z. A novel method of non-probabilistic reliability-based topology optimization corresponding to continuum structures with unknown but bounded uncertainties. Comput Methods Appl Mech Engrg 2017;326:573–95.
[54] Calafiore G, Campi M. Uncertain convex programs: randomized solutions and confidence levels. Math Program 2005;102(1):25–46.
[55] Campi M, Garatti S. The exact feasibility of randomized solutions of uncertain convex programs. SIAM J Optim 2008;19(3):1211–30.
[56] Campi MC, Garatti S. A sampling-and-discarding approach to chance-constrained optimization: Feasibility and optimality. J Optim Theory Appl 2011;148(2):257–80.
[57] Carè A, Garatti S, Campi M. Scenario min-max optimization and the risk of empirical costs. SIAM J Optim 2015;25:2061–80.
[58] Campi MC, Garatti S. Wait-and-judge scenario optimization. Math Program 2018;167(1):155–89.
[59] Grammatico S, Zhang X, Margellos K, Goulart P, Lygeros J. A scenario approach for non-convex control design. IEEE Trans Automat Control 2015;334–45.
[60] Campi MC, Garatti S, Ramponi FA. A general scenario theory for non-convex optimization and decision making. IEEE Trans Automat Control 2018;63(12):4067–78.
[61] Yang Y, Sutanto C. Chance-constrained optimization for nonconvex programs using scenario-based methods. ISA Trans 2019;90:157–68.
[62] Sadeghi J, de Angelis M, Patelli E. Frequentist history matching with interval predictor models. Appl Math Model 2018;61:29–48.
[63] Carè A, Ramponi FA, Campi MC. A new classification algorithm with guaranteed sensitivity and specificity for medical applications. IEEE Control Syst Lett 2018;2(3):393–8.
[64] Rocchetta R, Gao Q, Petkovic M. Scenario-based generalization bound for anomaly detection support vector machine ensembles. In *Proceedings of the 30th esrel -15th psam conference*, 2020.
[65] Calafiore GC, Campi MC. The scenario approach to robust control design. IEEE Trans Automat Control 2006;51(5):742–53.
[66] Rocchetta R, Crespo L, Kenny S. Solution of the benchmark control problem by scenario optimization. In *Proceedings of the ASME dynamic systems and control conference, DSCC, October*, 2019.
[67] Garatti S, Campi MC. Risk and complexity in scenario optimization. Math Program 2019;1–37.
[68] Miller BL, Wagner HM. Chance constrained programming with joint constraints. Oper Res 1965;13(6):930–45.
[69] Calfa B, Grossmann I, Agarwal A, Bury S, Wassick J. Data-driven individual and joint chance-constrained optimization via kernel smoothing. Comput Chem Eng 2015;78:51–69.
[70] Elçi O, Noyan N, Bülbül K. Chance-constrained stochastic programming under variable reliability levels with an application to humanitarian relief network design. Comput Oper Res 2018;96:91–107.
[71] Van Ackooij W. Chance constrained programming : with applications in energy management. (Theses), Ecole Centrale Paris; 2013.
[72] Boyd S, Vandenberghe L. Convex optimization. United States of America by Cambridge University Press; 2004.
[73] Uryasev S, Rockafellar RT. Conditional value-at-risk: Optimization approach. In: Uryasev S, Pardalos PM, editors. Stochastic optimization: algorithms and applications, Vol. 54. Boston, MA: Springer US; 2001, p. 411–35.
[74] Ahmed S. Convex relaxations of chance constrained optimization problems. Optim Lett 2014;8. http://dx.doi.org/10.1007/s11590-013-0624-7.
[75] Schildbach G, Fagiano L, Morari M. Randomized solutions to convex programs with multiple chance constraints. SIAM J Optim 2012;23. http://dx.doi.org/10.1137/120878719.
[76] Calafiore GC. Random convex programs. SIAM J Optim 2010;20(6):3427–64.
[77] Grooteman F. An adaptive directional importance sampling method for structural reliability. Probab Eng Mech 2011;26(2):134–41.
[78] Shang C, You F. A posteriori probabilistic bounds of convex scenario programs with validation tests. IEEE Trans Automat Control 2020.
[79] Dabbene F, Tempo R. Probabilistic and randomized tools for control design. In: The control systems handbook: control system advanced methods. 2010, second ed..
[80] Camp C, Farshchin M. Design of space trusses using modified teaching–learning based optimization. Eng Struct 2014;62–63:87–97.
[81] Lieu QX, Do DT, Lee J. An adaptive hybrid evolutionary firefly algorithm for shape and size optimization of truss structures with frequency constraints. Comput Struct 2018;195:99–112.
[82] Ho-Huu V, Nguyen-Thoi T, Le-Anh L, Nguyen-Trang T. An effective reliability-based improved constrained differential evolution for reliability-based design optimization of truss structures. Adv Eng Softw 2016;92:48–56.
[83] Truong V-H, Kim S-E. Reliability-based design optimization of nonlinear inelastic trusses using improved differential evolution algorithm. Adv Eng Softw 2018;121:59–74.
[84] Degertekin S. Improved harmony search algorithms for sizing optimization of truss structures. Comput Struct 2012;92–93:229–41.
[85] Vo-Duy T, Duong-Gia D, Ho-Huu V, Nguyen-Thoi T. An effective couple method for reliability-based multi-objective optimization of truss structures with static and dynamic constraints. Int J Comput Methods 2020;17(06):1950016.